CrossMark

Biogeochemical storm response in agricultural watersheds of the Choptank River Basin, Delmarva Peninsula, USA

Antti I. Koskelo · Thomas R. Fisher · Adrienne J. Sutton · Anne B. Gustafson

Abstract Stream discharge and chemistry (total suspended solids TSS, nitrogen N, and phosphorus P) were monitored for 15 months in six agricultural watersheds on the U.S. Mid-Atlantic coastal plain. Watersheds with similar land uses and a range of hydric soils were used to test the hypothesis that hydric soils generate large storm discharges due to low permeability, resulting in watershed areas with high loss rates of N, P, and TSS. To test the hypothesis, discharge was monitored continuously, and a flow separation method quantified the base and stormflow contributions. Another primary goal was to measure base and stormflow chemistry to quantify N, P, and TSS export. Baseflow chemistry was monitored monthly, and 31 storm events were sampled. Baseflow chemistry varied little over the 15 months, but stormflow chemistry was dynamic, with three major patterns: (1) TSS and particulate N and P had large, brief peaks during the rising limb of storm hydrographs; (2) phosphate and ammonium had broader peaks close to maximum discharges; and (3) nitrate concentrations decreased during the rising limb, slowly returning to pre-storm levels. Event water yields were correlated with volume-weighted mean concentrations (VWMs) of N, P, and TSS, providing a basis for estimating VWMs of unsampled events. Export coefficients ($kg\ ha^{-1}\ year^{-1}$) ranged over 22–33 for TN, 0.9–1.4 for TP, and 240–1140 for TSS. Most P and TSS export occurred during storms (71–99%), while most N export occurred during baseflow (52–84%). The discharge data did not support the hypothesis, and watershed slope, not hydric soils, was the major control on storm discharge. Surface ponding of water on hydric soils intercepted runoff, reducing the impacts of the low infiltration rates.

Keywords Hydric soils · Watershed slope · Flow separation · Volume-weighted mean · Choptank

A. I. Koskelo (✉) · T. R. Fisher (✉) ·
A. J. Sutton · A. B. Gustafson
Horn Point Laboratory, University of Maryland Center for
Environmental Sciences, 2020 Horn Point Road,
PO Box 775, Cambridge, MD 21613, USA
e-mail: koskeloantti@yahoo.com;
Antti.Koskelo@WSP.com

T. R. Fisher
e-mail: fisher@umces.edu

Present Address:
A. I. Koskelo
1001 Bishop St., ASB Tower, Suite 2400, Honolulu, HI 96813,
USA

Present Address:
A. J. Sutton
NOAA Pacific Marine Environmental Laboratory, 7600 Sand
Point Way NE, Seattle, WA 98115, USA

🖄 Springer

Introduction

Streams draining human-altered landscapes are at risk for poor water quality due to anthropogenic contaminants (e.g., Norvell et al. 1979; Novotny et al. 1985; Jordan et al. 1997a, b; Fisher et al. 2006; Powers et al. 2016). These contaminants include nitrogen (N), phosphorus (P), and total suspended solids (TSS), which can impair not only stream systems but also contribute to accelerated eutrophication and impaired ecosystem functioning in downstream receiving waters (e.g., NAS 2000; GOM Watershed Nutrient Task Force 2001; Kemp et al. 2005; Fisher et al. 2010). In agricultural regions, the primary sources of contaminants are animal husbandry and surface applications of fertilizer and manure for crop production (e.g., Correll et al. 1995; Denver et al. 2004; Beckert et al. 2011). These activities contribute anthropogenic N and P to the soil which leaches into ground and surface waters (e.g., Correll et al. 1995; Pionke et al. 1996; Jordan et al. 1997c; Fisher et al. 2006). During storms TSS is eroded from organic litter and mineral particles in the upper soil layer, as well as from stream bank erosion and re-suspended bedload from the bottom of the stream channel (Kuhnle et al. 1996; Thompson 2008).

Stream discharge consists of baseflow and stormflow components, which vary over different time scales. Baseflow originates from inflowing groundwater from the surficial aquifer during periods of dry weather and during storm events. The volume and chemistry of baseflow varies primarily over time scales of weeks to months (e.g., Fisher et al. 1998; Sutton et al. 2009; Vanni et al. 2001). In contrast, stormflow consists primarily of overland flow from the stream's contributing area during wet weather, and the volume and chemistry of stormflow vary over shorter time scales of minutes to hours due to rapid fluctuations in precipitation and overland flow (e.g., Correll et al. 1999; Fisher et al. 2006). While lasting only for brief periods, storm events can have a disproportionately large effect on seasonal or annual nutrient and sediment export due to high concentrations of N, P, and TSS and large discharge volumes that occur during storm events (e.g., Correll et al. 1999; Pionke et al. 2000; Gonzalez-Hidalgo et al. 2013).

Storm-driven transport of nutrients and sediment from agricultural areas to receiving waters has been the subject of many studies (e.g., Correll et al. 1995, 1999; Pionke et al. 1996, 2000; Jordan et al. 1997c; Vanni et al. 2001). These studies have shown that the most important drivers of in-stream nutrient concentrations (C) and export (E) are watershed properties and hydrologic factors. The important watershed properties include the proportion of agricultural land use, animal density, extent of riparian vegetated buffers, and soil permeability (e.g. well drained versus poorly drained). Hydrologic factors include stream flow characteristics such as flow duration curves (e.g., Mohamoud 2010), flow frequency distributions (e.g. Shields et al. 2008), or flow metrics such as the annual baseflow index (e.g. Jordan et al. 1997c). Other important hydrologic factors include the characteristics of a given storm event in terms of duration, precipitation type and intensity, total depth of precipitation, and antecedent dry period. Several reviews of the effects of stream discharge (Q) on in-stream concentrations (C) have demonstrated predictable patterns of watershed C-Q responses using watershed properties (Basu et al. 2010, Moatar et al. 2017; Musolff et al. 2017; Aguilera and Melack 2018).

In this study, the focus is on soil type, specifically the effects of hydric soils on stream discharge, with a second goal of quantifying the chemistry of storm events. Hydric soils were formed under conditions of saturation, flooding, or ponding persisting long enough during the growing season to develop anaerobic conditions in the upper part (Federal Register 1994). Hydric soils have slow drainage rates and require artificial drainage to allow agricultural crop growth. Yet hydric soils occur in a significant fraction of Coastal Plain areas, and it is important to understand the role of hydric soils in watershed biogeochemistry. Here we examine whether the low permeability of hydric soils affects stormwater quantity or quality at the small watershed scale on the Mid-Atlantic Coastal Plain of the U.S. Although studies have been conducted on the hydrologic effects of compacted, urban soils and impervious surfaces (e.g., Groffman et al. 2003; Pitt et al. 2004), the hydrologic impacts of hydric soils in agricultural areas are generally not well understood with regard to stormwater. The impetus of this study, therefore, is to contribute to a better understanding of how hydric soils affect storm-driven transport of nutrients and sediment to streams in agricultural watersheds. Our approach to studying the effects of soil permeability

was to monitor discharge and chemistry in six agricultural watersheds with varying amounts of hydric soils. Other important factors such as land use and rainfall were controlled in the experimental design, allowing us to isolate the impacts of hydric soils on discharge and transport of N, P, and TSS during storms. We hypothesize that watersheds with greater amounts of hydric soils generate more overland flow during storm events than infiltration of precipitation, resulting in greater stream discharges relative to watersheds with better drained, non-hydric soils.

Storms were sampled over a broad range of storm sizes, including two extreme events. This enabled an examination of the role of hydric soils at the upper end of the storm size distribution for the study area. This study also includes a systematic examination of volume-weighted mean N, P, and TSS concentrations in storm discharges using a flow separation program for small watersheds (Koskelo et al. 2012). This approach enabled an accurate estimate of annual stormflow volumes and chemistry relative to other approaches that do not utilize flow separation (e.g. Focazio and Cooper 1995; Buffam et al. 2001). The more accurate estimates of stormflow volumes and chemistry revealed strong statistical relationships between volume-weighted mean concentrations (N, P, and TSS) and event water yields which were used to quantify the contribution of unsampled storm events to nutrient and sediment export at the annual time scale.

Methods

Study area

This study was conducted in the Choptank Basin located on the Delmarva Peninsula in the Mid-Atlantic Coastal Plain of the U.S. (Fig. 1). The Choptank River drains the central portion of the Delmarva Peninsula, and tides and salt intrusion in the lower reach transform the river into the Choptank estuary, a tributary of Chesapeake Bay. The basin is primarily in the state of Maryland (MD) with a small portion of the headwaters extending into the state of Delaware (DE) (Fig. 1). The dominant land use is agriculture ($\sim 60\%$ of the basin by area; Fisher et al. 2006, 2010), primarily for production of corn, wheat, barley, and soybeans (McCarty et al. 2008). The basin contains numerous small to medium animal feeding operations for poultry and dairy operations, and waste materials and manure from the animal feeding operations are typically applied to corn and soybean fields as organic fertilizer (McCarty et al. 2008).

The Choptank Basin has soil series derived from parent material consisting of marine sands overlain by delta sands and gravel. In the U.S. Department of Agriculture (USDA) Soil Survey Geographic Database, five primary soil series in the Choptank cover 78% of the land area: Sassafras (29%; deep, well-drained sandy loams), Woodstown (24%; moderately well-drained loamy soils), Fallsington (14%; deep, poorly drained silts and clays), Elkton (6%; silty loams with a low permeability subsoil), and Pocomoke (6%; very poorly drained loam with a clay subsoil). Sassafras and Woodstown soils are non-hydric and primarily used for agriculture due to high permeability, whereas the others are poorly drained, hydric, and often interspersed with better drained soils. The well-drained soils are associated with the "well-drained upland" region in the southern Choptank near the estuary, which is characterized by low elevations and more incised stream channels (Phillips et al. 1993; Hamilton et al. 1993). The poorly drained soils, on the other hand, are associated with the "poorly drained upland" region, located in the higher elevation headwater area near DE where streams have limited channel incision.

The Delmarva Peninsula has a humid temperate climate with an average annual precipitation of 112 cm year^{-1} (Lee et al. 2001). While average rainfall is relatively evenly distributed throughout the year (Fisher et al. 2010), there are large seasonal fluctuations in evapotranspiration (ET) that vary with air temperature and insolation. Summers are characterized by high rates of ET, dry soils, and low water tables. As a result, a large portion of the rainfall occurring during the summer is absorbed by soil and returned to the atmosphere via ET, rather than moving to streams. During summers, baseflow discharges are low. In contrast, winters are marked by much lower rates of ET, resulting in elevated groundwater levels and soil moisture, higher baseflow discharges, and greater discharge from storm events (Fisher et al. 2010).

The study watersheds consist of six 3rd and 4th-order watersheds in the upper Choptank ranging from 14 to 27 km^2 in area (Table 1, Fig. 1). All of the
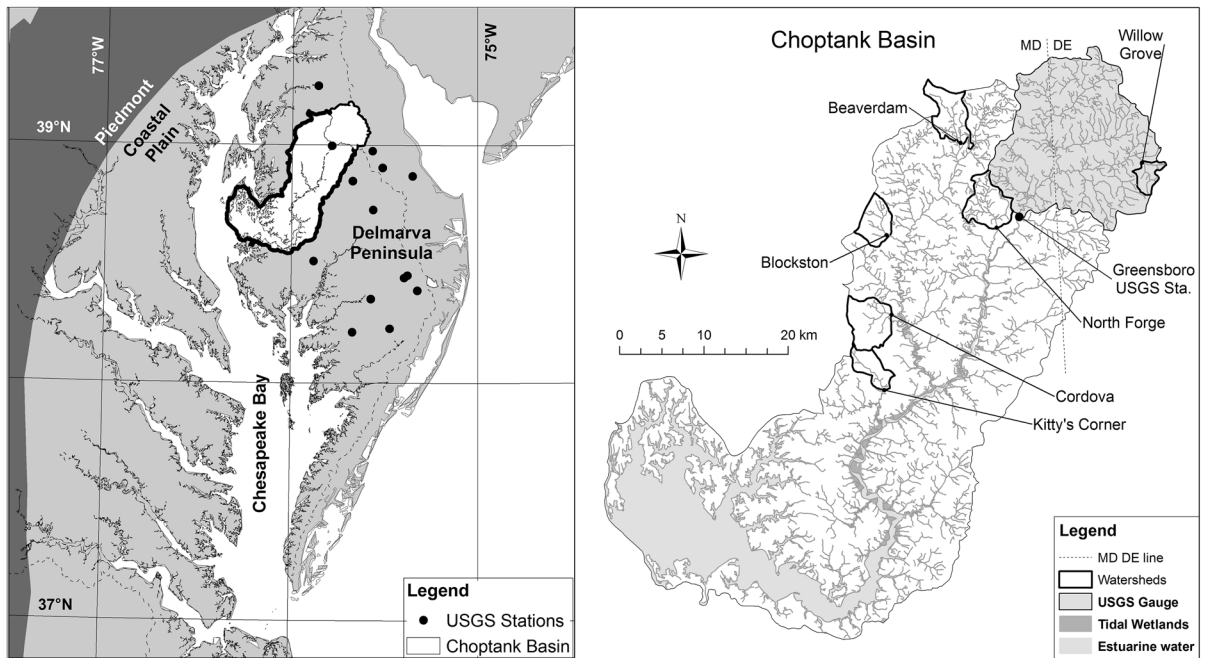
Fig. 1 Location of the Choptank Basin and supplementary USGS stations on the Delmarva Peninsula in the Mid-Atlantic region of the USA (left) and detailed map of the Choptank Basin (right). The study watersheds within the Choptank Basin are the clear polygons, and the Greensboro MD basin gauged by USGS is the shaded polygon

Table 1 Characteristics of the six study watersheds including size, slope, land use, and soil properties, ranked by % hydric soils

Watershed	Area (km²)	Watershed mean slope (% rise)	% Agriculture	% Forest	USDA hydrologic soil groups %				% Hydric soils	Primary hydric soil	% Watershed area
					A	B	C	D			
Cordova	27	0.70	76	18	60	22	17	1	15	Falsington	6
Kittys	14	0.70	65	32	52	22	23	2	26	Falsington	20
Blockston	17	0.40	71	28	2	40	20	38	34	Falsington	13
North Forge	24	0.41	67	31	33	17	30	21	51	Pocomoke	20
Beaverdam	22	0.26	67	32	1	28	6	66	64	Pocomoke	34
Willow Grove	15	0.31	34	58	0	1	2	97	97	Falsington	54

Hydrologic soil groups are A (very well drained), B (well-drained), and C (poorly drained), and D (very poorly drained). Hydric soils are found in hydrologic soil groups C and D, and the primary hydric soil series is listed. Percentages (except watershed slope) refer to percent of watershed area. Cordova and Willow Grove were only used for the hydrology analysis due to insufficient water chemistry data

watersheds except Willow Grove have predominantly agricultural land use representing 65–76% of the watershed areas. While land use is constrained within a narrow range, the watersheds have a broad range of hydric soils, ranging from 15 to 97% by area (Table 1). Hydric soils in the Choptank primarily

occur in low landscape positions where rain water naturally accumulates (known locally as "Delmarva Bays"), although they can also occur in areas with perched water tables and/or where soils are extremely fine-grained (silts and clays). Beaverdam, North Forge, and Willow Grove watersheds in the upper

headwaters are particularly high in hydric soils ($> 50\%$ by area).

This study includes a detailed evaluation of stream water chemistry and hydrology during storm events. Most of the watersheds were included in both the chemical and hydrologic analysis with the exception of Cordova and Willow Grove (Table 1) which were only evaluated for hydrology due to limited sampling for chemistry. To supplement the Choptank dataset, additional discharge data from over a dozen U.S. Geological Survey (USGS) stream gauging stations across Delmarva, including the one at Greensboro MD (Fig. 1), were obtained to provide a broader spatial context and a stronger statistical basis for testing the hypothesis of this study.

Measurements of precipitation and discharge

Precipitation and stream discharge were monitored continuously for 15 months (June 2006–August 2007, or 457 days) at the six Choptank watersheds (Table 1). Precipitation was measured as daily rainfall using data from 17 gauges that were well-distributed over a 50×50 km area in and near the study watersheds. Most of the data were collected using recording 20 cm diameter rain gauges at three reference stations in national monitoring networks: one at a nearby National Atmospheric Deposition Program site (NADP MD-13) and two at nearby National Weather Service sites (Dover DE and Royal Oak MD). Additional data were collected from six manual 10 cm rain gauges at the outlet of each watershed, seven Weather Underground personal weather stations, and one 20 cm recording gauge at the Horn Point Laboratory (HPL). The rainfall datasets for the 17 sites were evaluated to standardize the quality of the data and to produce a continuous record of daily precipitation (P_i, m day^{-1}) averaged across all stations for the duration of the monitoring period (Koskelo 2008). Briefly, the precipitation data were standardized by assuming that the measurements from the reference stations with better equipment and QC procedures were more representative of precipitation totals than the supplemental sites. An analysis by Koskelo (2008) found that precipitation totals of some supplemental sites deviated significantly from the reference stations due to instrument or catch bias, and therefore the data from these sites were adjusted to match the average rainfall total of the three reference stations during the study period. This approach retained the temporal and spatial variations recorded by the gauges but removed instrument or catch bias from the non-reference sites. Data gaps at the supplemental sites were filled using average values from all other sites.

Stream stage (m) and temperature (°C) data were collected at 30-min intervals at the watershed outlets. We used Solinst model 3001 data loggers attached to the inside of a cinder block anchored in the stream bottom. The blocks stabilized the loggers in place and provided protection from storm debris. Corrections for barometric pressure were applied to the stage data using a separate reference barologger (Solinst model 3001) exposed to the atmosphere at HPL $\sim$ 50 km from the watersheds. A staff gauge installed near the submerged data loggers provided visual records of stream stage, and a linear relationship with a slope of $\sim$ 1 was developed between the staff gauge readings and logger records for each watershed.

Stream discharge was measured as stage converted to discharge using rating curves developed for each watershed. The rating curves were developed for each watershed by measuring discrete flow rates over a wide range of stages over a 2–3 year period, including the period of study (June 2006–August 2007). Discharge was primarily measured with a Pygmy analog velocity meter using the cross-sectional, area-velocity method; however, during high discharges when wading the stream was not feasible, an RD Instruments (Poway, CA) StreamPro Acoustic Doppler Current Profiler was used. Overlapping discharge data from the two instruments were consistent, and the stage-discharge rating curves were all highly significant ($p < 0.0001$) exponential or linear/exponential functions with r^2 values of 0.94–0.99 (e.g., Fig. 2). Each rating curve had at least 15 data points representing paired stage and discharge measurements.

The 30-min stage data recorded by loggers at the outlet of each watershed were processed as follows. First, stage data were converted to instantaneous discharge (Q, m^3 s^{-1}) using the rating curves and aggregated to daily discharge for each day i of the study period (Q_i, m^3 day^{-1}). The daily discharges were divided by watershed area (A, m^2) to produce daily water yields (Y_i, m day^{-1}), which allowed a direct comparison of water yields with precipitation (P_i, m day^{-1}) and among watersheds of different sizes. This process resulted in a continuous daily record of

Fig. 2 Example of stage-discharge rating curve for the Kitty's Corner watershed, a discontinued USGS watershed, showing data points collected by Horn Point Laboratory (HPL) and by the U.S. Geological Survey (USGS). A linear regression was fit to the data points up to 0.7 m of data points > 0.7 m when water overtopped the dam depth when water flowed only through a notch in the dam, and an exponential curve was fit to data points > 0.7 m when water overtopped the dam
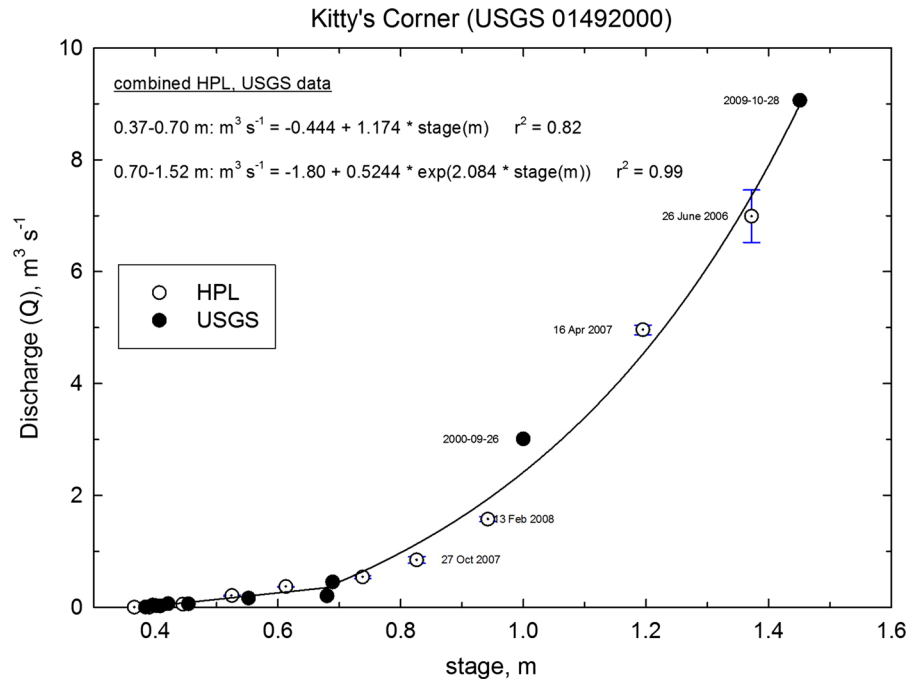
precipitation, discharge, and water yield for each watershed during the 15-month monitoring period.

Identifying individual storm events

Storm events were identified using the computer program Sliding Average with Rain Record (SARR, Koskelo et al. 2012). The program identifies storm events based on a flow classification system in which all Q_i in the discharge record are categorized as either 100 percent baseflow during dry weather ($Q_{B,i}$) or as a mixture of base and storm discharge during wet weather. SARR examines the P_i and Q_i records to identify inflection points in Q_i which indicate the beginning or end of a storm event. For days identified as being part of a storm event, the baseflow component $Q_{B,i}$ is determined via linear extrapolation between discharge data points that were previously identified as marking the beginning and end of the storm event. The remainder of the discharge is considered to represent direct storm runoff or $Q_{S,i}$ (where $Q_{S,i} = Q_i - Q_{B,i}$).

The output of SARR is a table summarizing precipitation and discharge data for each identified storm event in the period of record. The output table includes (1) start and end dates for each event j; (2) total rainfall for each event j ($P_{e,j}$, m event^{-1}), computed as the sum of P_i during event j; (3) total

discharge (base + storm flows) for each event j ($Q_{e,j}$ m^3 event^{-1}), computed as the sum of Q_i during event j; and (4) the stormflow volume for event j ($Q_{S,j}$ m^3 event^{-1}), computed as the sum of $Q_{S,i}$ during event j. Q terms were normalized by watershed area to produce water yields ($Y_{e,j}$, $Y_{S,j}$). For more information on SARR, see Koskelo et al. (2012). Table 2 summarizes symbol definitions and units used throughout this paper.

Sample collection

Monthly baseflow samples were collected manually from June 2006 to August 2007 at the watershed outlets. Samples were collected following 3 days of dry weather to ensure that groundwater chemistry was represented. The baseflow chemistry data used here are part of a larger dataset collected in the Choptank watersheds from 1986 to the present. The data are summarized in Table 3, and subsets of the data have been previously analyzed and published (Norton and Fisher 2000; Fisher et al. 2006, 2010; Koskelo 2008; Sutton et al. 2009, 2010). The baseflow data are used to compare with the stormflow data, and to estimate total annual baseflow export of N, P, and TSS. Sutton et al. (2010) showed that monthly sampling of

Table 2 Symbols used in this manuscript, with their units and definitions

Symbol	Units	Definition
A	m^2	Watershed area
P_i	$m\ day^{-1}$	Daily precipitation on day i (i = 1 − 457)
$P_{e,j}$	m	Cumulative daily precipitation during event j, $P_{e,j} = \Sigma P_i$ for i within event j (j = 1 − 99)
$T_{e,j}$	°C	Average event stream temperature measured at 30 min intervals by the Levelogger
Q	$m^3\ s^{-1}$	Instantaneous (30 min) discharge calculated from the stage records and rating curves
Q_k	$m^3\ s^{-1}$	Average of 4 nearest 30-minute discharge measurements associated with kth storm sample (baseflow + stormflow), k = 1–24
Q_i	$m^3\ day^{-1}$	Daily discharge on day i of the study period
$Q_{B,i}$	$m^3\ day^{-1}$	Baseflow component of Q_i estimated by SARR, occurs every day
$Q_{S,i}$	$m^3\ day^{-1}$	Stormflow component of Q_i estimated by SARR, $Q_{S,i} = 0$ on baseflow days
$Q_{e,j}$	m^3	Cumulative event volume (baseflow + stormflow) during event j, $Q_{e,j} = \Sigma Q_i$ for i within event j
$Q_{S,j}$	m^3	Cumulative stormflow volume during event j, $Q_{S,j} = \Sigma Q_{S,i}$ for i within event j
Y_i	$m\ day^{-1}$	Daily water yield on day i, Q_i normalized per ha of watershed area (A)
$Y_{B,i}$	$m\ day^{-1}$	Baseflow component of Y_i identified by SARR for day i
$Y_{S,i}$	$m\ day^{-1}$	Stormflow component of Y_i identified by SARR for day i
$Y_{e,j}$	m	Cumulative water yield of baseflow + stormflow during event j, $Y_{e,j} = \Sigma (Y_{B,i} + Y_{S,i})$ for i within event j
$C_{B,i}$	$g\ m^{-3}$	Measured concentration in a monthly baseflow sample collected manually
C_k	$g\ m^{-3}$	Measured concentration in kth composite of 2, one-hour storm samples collected by the ISCO sampler (base + storm water)
VWM_j	$g\ m^{-3}$	Volume-weighted mean concentration during event j (base + storm water, Eq. 1)
$VWM_{S,j}$	$g\ m^{-3}$	Calculated volume-weighted mean for the stormflow component of event j (Eq. 3)
SE_{VWM}	$g\ m^{-3}$	Standard error of VWM_j (Eq. 4)
Δt	h	Difference in time between the peak or nadir of sediment or nutrient concentrations relative to peak flow (Fig. 3)
$E_{B,i}$	$kg\ day^{-1}$	Baseflow export on day i, $E_{B,i} = Q_{B,i} \times C_{B,i}$
E	$kg\ year^{-1}$	Total annual export of TSS, N, or P in both baseflow and stormflow, $E = E_B + E_S$
E_B	$kg\ year^{-1}$	Annual export of TSS, N, or P in baseflow, $E_B = \Sigma\ Q_{B,i} \times C_{B,i}$
E_j	kg	Export of TSS, N, or P in storm j
E_S	$kg\ year^{-1}$	Annual export of TSS, N, or P in stormflow, $E_S = \Sigma\ Q_{S,j} \times VWM_j$
Y	$kg\ ha^{-1}\ year^{-1}$	Total annual export of TSS, N, or P in both baseflow and stormflow (E) normalized per ha of watershed area (A)
Y_B	$kg\ ha^{-1}\ year^{-1}$	Baseflow component of Y
Y_S	$kg\ ha^{-1}\ year^{-1}$	Stormflow component of Y

baseflow in the Choptank watersheds is adequate to resolve seasonal variations in baseflow chemistry.

Storm water samples were collected for 31 storm events at four of the watersheds (Kitty's Corner, Blockston, North Forge, and Beaverdam; Table 1) from June 2006 to August 2007. The samples were collected using Teledyne ISCO (Lincoln, NE) model 3700 automated samplers installed at the outlet of each watershed where baseflow samples were collected. A strainer at the end of the ISCO sampling tube prevented clogging of the tube, and the strainer was mounted on top of the cinder block housing the stage logger about 15–20 cm above the stream bottom to avoid collecting bedload. The ISCO samplers were programmed to collect 500 ml samples hourly and to combine every two samples into a single 1000 ml bottle, resulting in 24 samples (each representing 2 h) over a 48 h period. This sampling frequency is

Table 3 Summary of baseflow chemistry in the four Choptank watersheds with sufficient sampling for water chemistry

Watershed	NH_4^+	NO_3^-	TN	PO_4^{3-}	TP
Kitty's Corner	15 ± 3	210 ± 6	269 ± 7	1.1 ± 0.1	2.1 ± 0.1
Blockston	7.8 ± 1.9	468 ± 10	541 ± 11	0.75 ± 0.04	1.4 ± 0.1
Beaverdam	3.5 ± 0.5	283 ± 5	328 ± 6	0.68 ± 0.09	1.6 ± 0.1
North Forge	5.8 ± 1.4	316 ± 8	366 ± 9	0.70 ± 0.07	1.5 ± 0.1

Samples were collected monthly during 1986–1987 and 2003–2015. For analyses see Norton and Fisher (2000), Fisher et al. (2006, 2010), Koskelo (2008), and Sutton et al. (2009, 2010). All concentrations are in μM (mean $\pm$ SE)

consistent with the 1–2 day hydrologic response times of the watersheds for small to moderate storms (< 2.5 cm per event, Fisher et al. 2010). The ISCO sampling program was triggered using a small sensor (Teledyne ISCO model 1640 liquid level actuator) mounted $\sim$ 1 cm above the stream surface. After the storm, the samples were retrieved from the field immediately, stored at 4 °C in the dark, and processed within a few days. Acid preservatives were not used in the sample bottles to avoid dissolution of particulate nutrients (Jordan et al. 1997a).

Laboratory methods

Both the baseflow and stormflow samples were tested for various types of N and P, and (in the case of the storm samples) for TSS. The following symbols are used to indicate water quality constituents that were measured in the samples: dissolved reactive phosphate (PO_4^{3-}), particulate phosphorus (PP), total dissolved phosphorus (TDP), total phosphorus (TP), dissolved ammonium (NH_4^+), dissolved nitrate + nitrite (NO_3^-), particulate nitrogen (PN), total dissolved nitrogen (TDN), total nitrogen (TN), and TSS. The stormflow samples were tested for all of the above while the baseflow samples were only tested for PO_4^{3-}, TP, NH_4^+, NO_3^-, and TN.

Water samples were processed using standard laboratory methods. Samples were quantitatively filtered with 0.4 μm Whatman Glass Fiber Filters (GFF), and the filtrate was tested for dissolved nutrients using a Lachat Autoanalyzer at the USDA's laboratory in Beltsville, MD. For TP, TDP, TN, and TDN, the samples were digested using the persulfate digestion method (Valderrama 1981) to oxidize all forms of P and N to PO_4^{3-} and NO_3^- with an

efficiency of $\sim$ 80% for TDP and > 95% for TDN using known organic compounds (Koskelo 2008).

The GFF filters from the quantitative filtration of the storm samples were analyzed for PP, PN, and TSS. For PP, the filters were combusted at high temperature (450 °C) to remove organic matter and boiled in hydrochloric acid to solubilize the PO_4^{3-} residue (Andersen 1976). The liberated PO_4^{3-} was measured using the ascorbic acid method (Strickland and Parsons 1972). PN in the storm samples was measured with an elemental analyzer (Exeter Analytical model CE-440) at HPL's Analytical Services Lab. Due to financial and time constraints, only selected samples corresponding to the rising limb, peak, and falling limb portions of the hydrographs were tested for PP and PN. TSS was measured as the change in dry weight of the filter divided by the water volume. TN and TP in stormflow were calculated as TDN + PN and TDP + PP.

Both the baseflow and stormflow samples were also tested for specific electrical conductivity (SEC, μmho cm^{-1}) and pH. The electrical conductivity and temperature of samples was measured using a Yokogawa model SC82 probe, and conductivity was converted to SEC at 25 °C using a temperature coefficient of 0.023 $°C^{-1}$ derived from samples collected at the nearby USGS stream gauging station at Greensboro, MD (Fig. 1, Fisher et al. 1998). The pH of the samples was measured with a VWR Symphony model SP70P probe calibrated with pH 4 and 7 standards.

Volume-weighting of the storm samples

For each storm event j, the volume-weighted mean concentrations (VWM_j, g m^{-3}) of N, P, TSS, SEC, and pH were computed. The measured concentrations in each of the 24 ISCO storm samples (C_k) were

Fig. 3 a Example hydrograph and chemographs from a November 2006 event showing integration of the 30 min discharge (Q) data and the composited 2 h chemistry data (C_k) to compute volume-weighted means (VWM_j). **b** Calculation of the time difference (Δt, arrow) between the peak concentration and the peak discharge. Δt can be negative (preceding the discharge peak, as for PP) or positive (following the discharge peak, as for NO_3^-, shown in Fig. 4
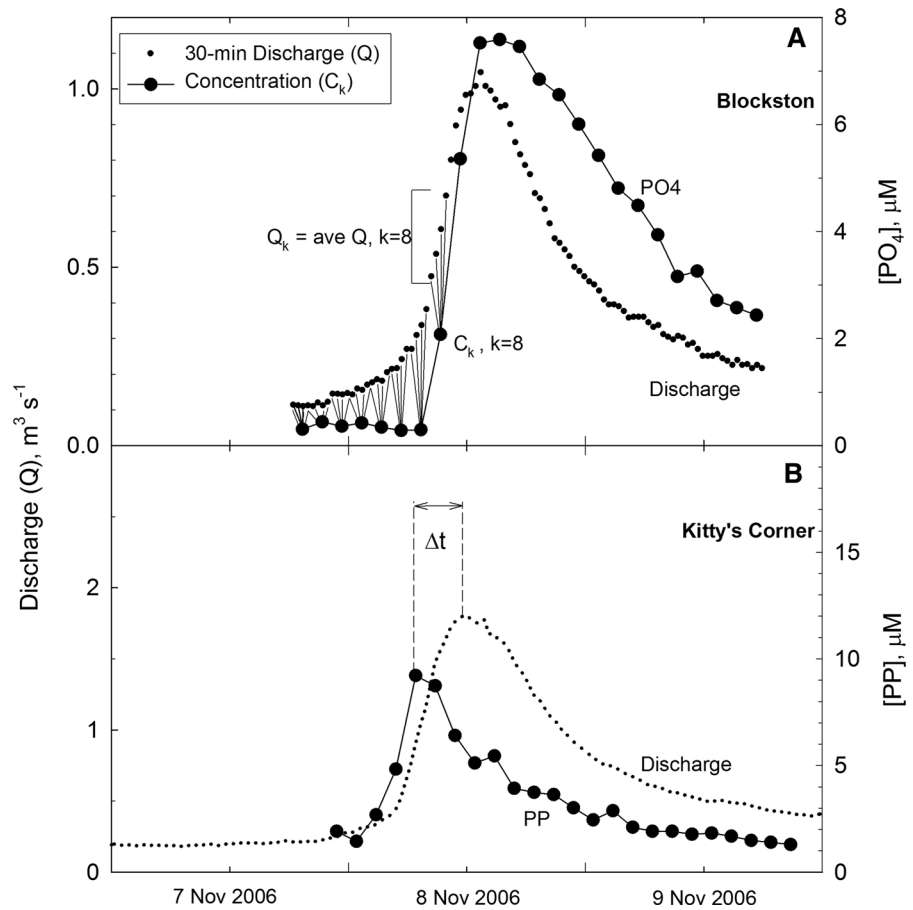
multiplied by the average of the four closest 30-min discharge values associated with each sample (Q_k, $m^3 \ s^{-1}$, Fig. 3a). The sum of the product of concentration and discharge was normalized by the total discharge during the event, as follows:

$$VWMj = \frac{\sum_{k=1}^{24} (C_k \times Q_k)}{\sum_{k=1}^{24} Q_k} \quad (1)$$

For pH, the measurement was de-logged before volume-weighting and then re-logged. In a few cases only selected storm samples were analyzed due to financial constraints and the sample mid-point method (Press et al. 2007) was used to estimate $VWMj$.

The values of VWM_j (Eq. 1) were based on the ISCO storm samples, which were a mixture of baseflow and storm flow (Fig. 4c). To separate VWM_j into its baseflow ($C_{B,j}$) and stormflow chemistry components $VWM_{S,j}$), we used the baseflow and stormflow discharge components $Q_{B,j}$ and $Q_{S,i}$ ($m^3 \ day^{-1}$) provided by the SARR flow separation

program. We used the $C_{B,i}$ value closest in time to estimate $C_{B,j}$, and $VWM_{S,j}$ was derived from the following mass balance:

$$(VWM_j \times \Sigma Q_k) = (C_{B,i} \times \Sigma Q_{B,i}) + (VWM_{S,j} \times \Sigma Q_{S,i}) \quad (2)$$

From this equation, $VWM_{S,j}$ was solved as follows:

$$VWM_{S,j} = \left[(VWM_j \times \Sigma Q_k) - (C_{B,i} \times \Sigma Q_{B,i}) \right] / \Sigma Q_{S,i} \quad (3)$$

Equation 3 was used to quantify both a volume-weighted mean concentration ($VWM_{S,j}$) reflecting overland flow, and a baseflow concentration reflecting groundwater inputs to the stream. The error associated with VWM terms was based on the sample variance (Zar 1999), as follows:

$$SE_{VWM} = \frac{\sqrt{\sum_{k=1}^{n} \frac{(C_k - VWM)^2}{n-1}}}{\sqrt{n}}, \quad (4)$$
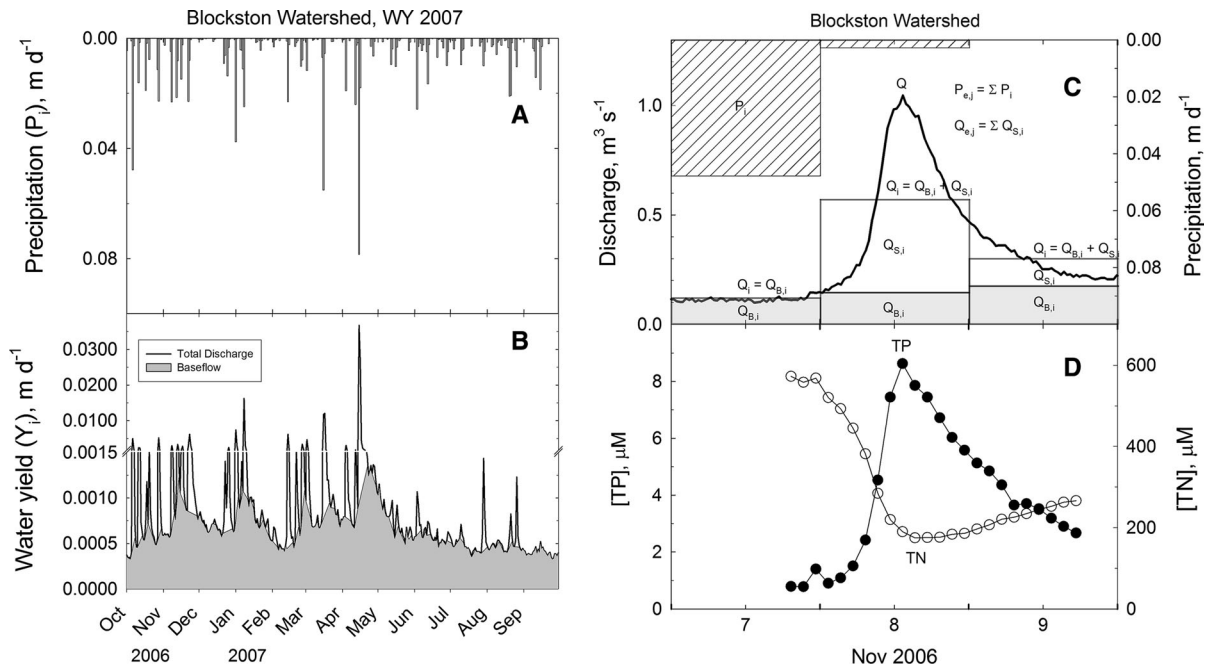
Fig. 4 **a** Daily rain (P_i) at Blockston watershed for WY 2007. Note the inverted y axis. **b** Daily water yield (Y_i) at Blockston watershed separated into baseflow ($Y_{B,i}$ shaded) and stormflow ($Y_{S,i}$ clear) components using the SARR program. **c** Example of a single storm event at Blockston watershed in November 2006 showing daily precipitation (P_i), daily flow (Q_i), and the 30-min stream discharge (Q). Q_i was separated by SARR into base ($Q_{B,i}$) and storm ($Q_{S,i}$) components. **d** Stream concentrations (C_k) of total P (TP, filled circles) and total N (TN, open circles) during the storm event shown in (**c**)

where SE_{VWM} = standard error associated with VWM, n = the number of samples collected during a storm event (usually 24), and C_k is defined above.

Event temperature and timing of peak concentrations

The mean stream temperature during each storm event j ($T_{e,j}$, °C) was used to evaluate effects of water temperature on concentrations of N, P and TSS. $T_{e,j}$ was calculated as the average of 30-min temperature readings recorded in the stream during each SARR-identified storm event j.

The difference in timing between peak discharge and peak concentrations was calculated for all sampled storm events to indicate the rates at which N, P, and TSS were flushed from the watershed during storms. The time difference (Δt, h) was calculated as the number of hours between the discharge peak and the concentration peak. Positive Δt values indicated that concentrations peaked after discharge, while negative values indicated the opposite. In some cases,

more than one value of Δt was calculated because of multiple peaks in the storm hydrograph. For analytes which decreased in concentration during stormflow (e.g., NO_3^-), the nadir rather than the peak was used to calculate Δt. Examples are shown in Fig. 3.

Calculation of annual export coefficients

Total annual export of TSS, TN, and TP (E, kg year^{-1}) was calculated as the sum of baseflow export (E_B, kg year^{-1}) and stormflow export (E_S, kg year^{-1}) for each watershed. Annual baseflow export (E_B) was summed from daily baseflow export ($E_{B,i}$, kg day^{-1}), which was computed as the product of daily baseflow discharge ($Q_{B,i}$, m^3 day^{-1}) and the monthly baseflow concentration closest in time ($C_{B,i}$, g m^{-3}). To estimate annual baseflow export (E_B, kg year^{-1}), the daily baseflow export ($Q_{B,i} \times C_{B,i}$) was summed over the 457 day monitoring period, scaled to one year, and converted to kg. For comparisons among watersheds, E_B was normalized by watershed area (A, converted to ha) to produce N, P, and TSS annual export coefficients for baseflow (Y_B, kg ha^{-1} year^{-1}).

Annual stormflow export (E_S, kg year^{-1}) was computed by summing the individual storm export of TN, TP, and TSS for all sampled and unsampled storm events within the monitoring period. During each sampled event j, $VWM_{S,j}$ was calculated using Eq. 3, or was derived from the relationships described below (Fig. 9) for unsampled events. The individual storm export during event j ($E_{S,j}$, g event^{-1}) was estimated as the product of $VWM_{S,j}$ and $Q_{S,j}$. Annual stormflow export (E_S, kg year^{-1}) was computed as the sum of all individual storm events, scaled to one year, converted to kg, and normalized by watershed area (ha) to produce annual N, P, and TSS export coefficients for stormflows (Y_S, kg ha^{-1} year^{-1}).

A few larger events were longer than the 48-h sampling period. The calculated VWM_j was not representative of the entire event, and the discharge volume associated with the unsampled portion of the hydrograph was used to estimate a second VWM using the empirical relationships in Fig. 9. The first VWM (based on sampling) was multiplied by the sampled discharge volume, and the second VWM (estimated using Fig. 9) was multiplied by the unsampled discharge volume. The partial export values were added to obtain the total event export.

Statistical analyses

Statistics and graphs were made in SigmaPlot v12.5. Failure of a normality test resulted in use of a non-parametric test, and parsimonious selection of statistical models was based on the Akaike Information Criterion (AIC, Akaike 1973). Complex models were chosen over simpler models if the AIC values were $\pm$ 7 (Burnham and Anderson 2002). The following symbols were used for statistical significance: NS = not significant ($p > 0.05$), *$p < 0.05$, **$p < 0.01$, ***$p < 0.001$.

The hypothesis that hydric soils generate more storm discharge due to their low permeability was tested using a correlation analysis. %hydric soils in each watershed (both the Choptank watersheds and USGS watersheds) was determined using the USDA SSURGO database. For each watershed the % hydric soils was compared to annual stormflow, annual baseflow, and total water yields (m year^{-1}) to test our hypothesis that the low permeability of hydric soils enhances overland flow. To test the alternative hypothesis that mean watershed slope controls storm discharge, we calculated mean watershed slope for the Choptank and USGS watersheds using ArcMap v10.1 and a 1-m resolution Digital Elevation Model of the Delmarva Peninsula obtained from MD iMAP Mapping and GIS Data Portal (imap.maryland.gov/Pages/default.aspx).

Results

Storms and hydrology

Annual precipitation over the 15-month study period (June 2006–August 2007) was 1.07 m year^{-1}. This is

Fig. 5 Water budgets for six watersheds in the Choptank Basin showing the baseflow, stormflow, and watershed storage/ET components. The sum of all the components equals the annual precipitation of 1.07 m year^{-1}
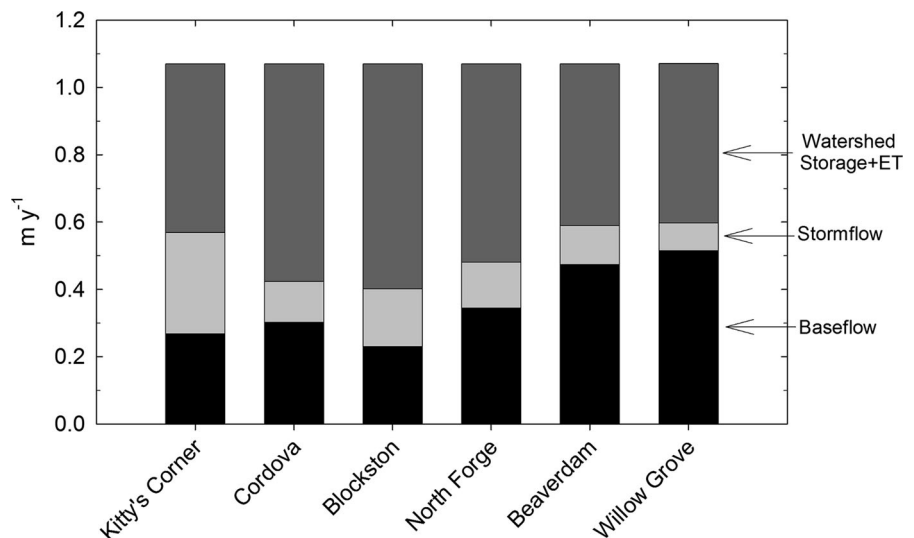
similar to the 20-year average precipitation for the Choptank Basin (1.12 m year^{-1}, Fisher et al. 2010). Although there were drought periods in this study, especially in mid-summer to early fall of 2006, significant rains occurred in other seasons to restore the annual precipitation total to approximately average levels. During the entire monitoring period, a total of 92–98 individual storm events were identified using SARR at the Blockston and Beaverdam watersheds (Fig. 1) with complete discharge records. However, fewer storms were identified at the other watersheds due to data gaps in the hydrologic record associated with logger malfunctions. At these watersheds, we recorded only 58–85 events due to the shorter periods of record.

Over the monitoring period, storms varied in size from 0.01 to 0.19 m of precipitation reflecting the large range of storm sizes during this study. Smaller events < 0.02 m were more frequent, representing 65% of the total number of storms. Two extreme events occurred in June 2006 (0.19 m of rain) and April 2007 (0.10 m of rain), and both resulted in flooding of roads and streams across the Delmarva Peninsula. The combined rainfall for these two events (0.29 m) made up 27% of the annual rainfall. The associated peak discharges at the USGS station at Greensboro MD were 70 m^3 s^{-1} (June 2006 storm) and 118 m^3 s^{-1} (April 2007 storm), which are in the 99th percentile of historical peak flows since 1948 and

Fig. 6 A storm event sampled at Blockston watershed showing **a** TSS concentrations, **b** PO$_4^{3-}$ concentrations, and **c** NO$_3^-$ concentrations during a peak in stream discharge
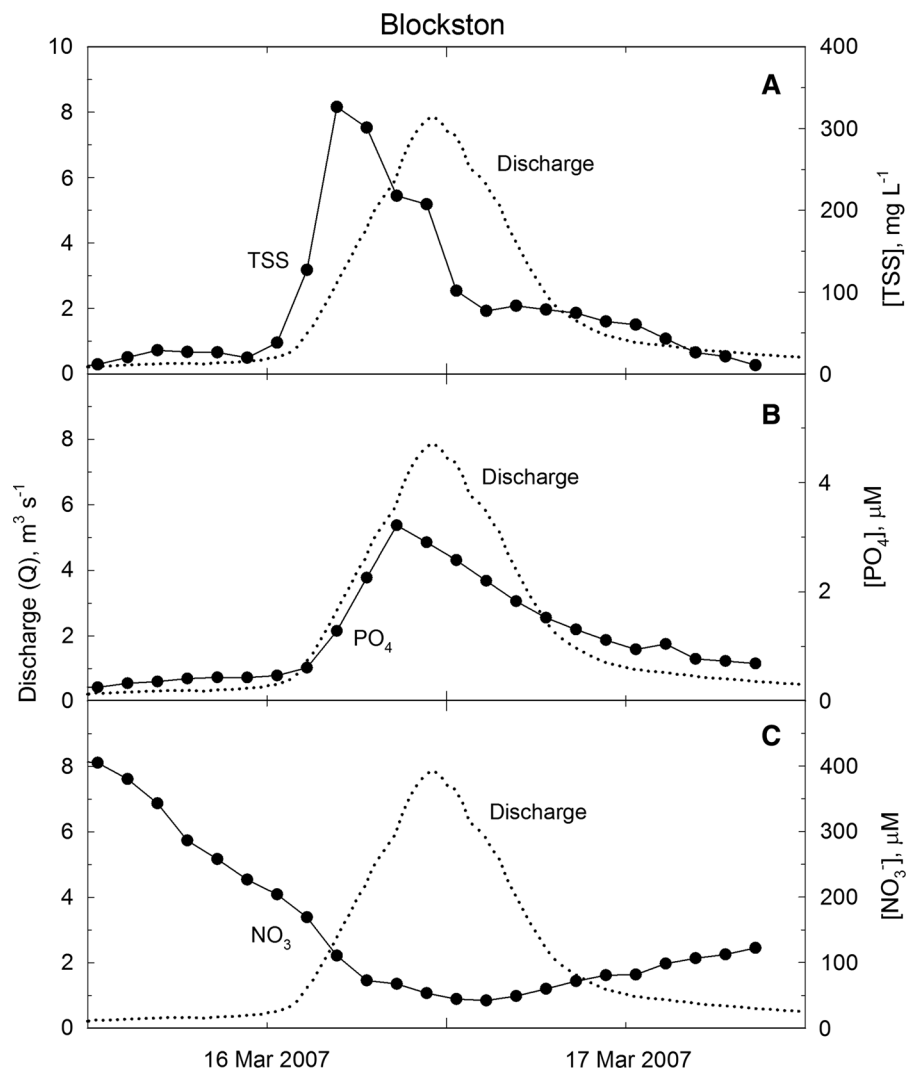
Table 4 Timing of peak concentrations for various parameters (rows) relative to peak discharge (in hours) for the four study watersheds and for all watersheds combined (last two columns)

Parameter	Hours before or after peak discharge									
	Kitty's Corner		Blockston		Beaverdam		North Forge		All watersheds	
	Mean	SE	Mean	SE	Mean	SE	Mean	SE	Mean	SE
PO$_4$-P	3.8	1.2	2.8	2.5	9.2	3.7	7.9	3.0	5.7	1.4
NH$_4$-N	4.1	2.8	− 3.4	3.0	− 0.3	3.9	− 2.1	1.3	− 0.5	1.5
NO$_3$-N	5.7	1.3	4.1	1.2	6.6	4.0	2.4	0.6	4.5	1.0
Cond (25)	7.3	3.2	0.9	1.2	6.0	4.1	0.4	1.3	3.3	1.3
pH	− 1.3	3.4	− 6.6	4.8	1.1	3.3	6.7	5.3	− 0.4	2.3
TSS	− 2.8	0.8	− 5.3	1.4	7.7	4.0	− 2.1	1.1	− 1.3	1.2
PP	− 2.4	2.2	− 4.3	1.6	5.6	4.6	− 0.6	3.5	− 1.7	1.3
PN	− 4.3	1.2	− 4.2	2.1	6.3	4.0	− 2.3	3.1	− 1.8	1.6
TDN	7.2	1.9	2.6	1.2	7.5	3.4	3.9	1.9	5.2	1.1
TN	7.0	2.1	7.3	2.4	0.3	1.7	− 3.0	3.1	3.5	1.7
TDP	4.7	1.0	2.3	3.0	11.2	5.0	4.7	1.6	5.3	1.5
TP	− 0.2	1.9	− 1.9	2.8	8.3	2.4	0.4	3.5	0.7	1.7

Negative numbers indicate that the concentrations peaked before discharge and positive numbers mean the concentrations peaked after discharge

were among the highest peak flows recorded during the previous decade.

A total of 31 storm events were sampled at the four watersheds with adequate chemistry data (7–10 storms at Kitty's Corner, Blockson, North Forge, and Beaverdam). The sampled storms represented ∼ 20% of the storms recorded at each watershed over the 15-month monitoring period. For the sampled events, rainfall totals ($P_{e,j}$) ranged from 0.01 to 0.19 m, while storm event water yields ($Y_{e,j}$) ranged from 0.01 to 0.07 m. As described above, major events occurred in June 2006 and April 2007, both of which were sampled, and the remaining sampled storms were well distributed seasonally during summer, fall, winter, and spring (Fig. 4a).

In general, storm hydrographs of 30-min discharge (Q) at the Choptank watersheds had a characteristic shape (Fig. 4c). The initial part of the storm consisted of a steep rising limb (usually < 12 h for a moderate size storm), followed by a brief peak (< 2 h), and then a long gradual tail (the falling limb) lasting for 1–3 days. During the two extreme events, the falling limb continued for almost 1 week. After each storm passed, the streams often returned to a higher baseflow than just prior to the storm (e.g., Fig. 4c), indicating recharge of the local groundwater. This effect was especially pronounced in the late fall, winter, and early spring when soils were nearly saturated and the water table was high.
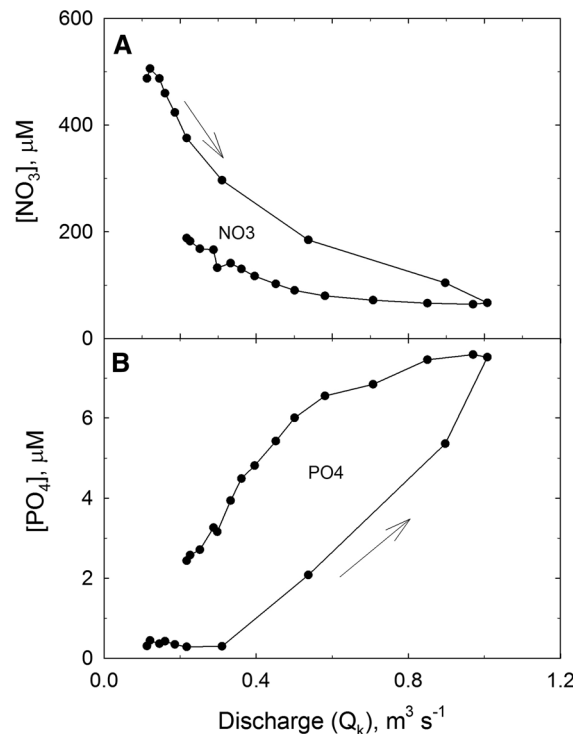
Fig. 7 Example of hysteresis plots of sample concentration (C_k) versus discharge (Q_k). **a** Nitrate followed a clockwise hysteresis (arrow indicates time going forward), while **b** phosphate followed a counter-clockwise hysteresis

Annual water budgets for the six watersheds are summarized in Fig. 5. On average ∼ 50% of the total annual precipitation was discharged as measured
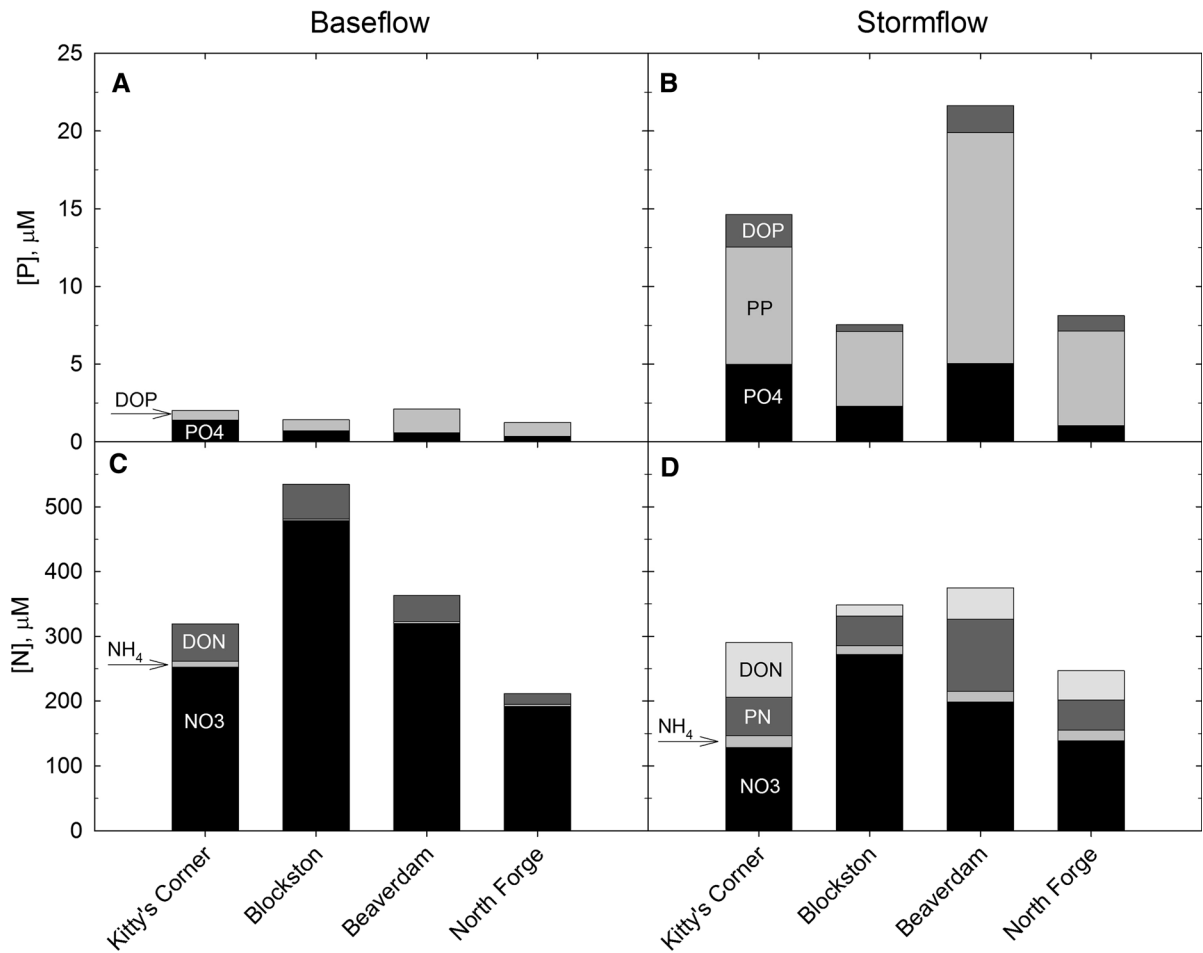
Fig. 8 Constituents of TN and TP in baseflow and stormflow samples: **a** P concentrations during baseflow, **b** P concentrations during stormflow, **c** N concentrations during baseflow, and **d** N concentrations during stormflow. Bars are labeled showing the different fractions of total N and P

baseflow or stormflow, while the other (unmeasured) half was assumed to be lost to the atmosphere as ET or stored as soil water or groundwater. Across the watersheds, baseflow and stormflow represented 33% and 14% of annual rainfall, respectively. As a fraction of total annual discharge, baseflow and stormflow represented 69% and 31%, or approximately two-thirds and one-third. However, there was clearly some variation among the watersheds. For example, the Kitty's Corner watershed in the well-drained southern part of the basin had almost four times the amount of stormflow as Willow Grove (0.30 m versus 0.08 m year^{-1}) in the poorly drained northern headwaters. Furthermore, Willow Grove and Beaverdam, the watersheds with the highest percentage of hydric soil (Table 1), had the smallest amounts

of storm flow (Fig. 5). This hydrologic behavior does not support our hypothesis and is explored further below. In addition to the observed spatial variations, the stormflow discharge volumes for individual events varied seasonally, and during the cooler months (October–April), the watersheds generated about twice as much stormflow compared with the warmer months (May to September, see Fig. 4b).

Total annual water yields (baseflow + stormflow) for the six watersheds during the study period ranged from 0.39 to 0.59 m year^{-1} (mean $\pm$ se = 0.51 $\pm$ 0.04 m year^{-1}). This large variation is likely due to the spatial variability in precipitation associated with the two large storm events (June 2006 and April 2007) included in this data set, as well as measurement errors. For comparison, the water yield at the nearby

USGS stream gauging station at Greensboro (Fig. 1) over the same time period was 0.39 m year^{-1}, while the 60-year mean water yield at Greensboro was 0.43 m year^{-1} (Fisher et al. 2010).

Comparison of baseflow and stormflow chemistry

Nutrient and sediment concentrations varied significantly over hourly time scales during storm events and generally followed one of three patterns. The first pattern was a large but brief peak in concentrations on the rising limb of the hydrograph followed by a rapid return to pre-storm concentrations. This pattern was typical of the particulates (PP, PN, and TSS; Fig. 6a).

The second common pattern was a moderate increase in concentrations with a broader peak close to the maximum discharge and a gradual return to pre-storm concentrations on the falling limb. This pattern was typical of TP, PO_4^{3-}, and NH_4^+ (Figs. 3a, 4d, 6b). In the third pattern, concentrations decreased during stormflows and very slowly returned to pre-storm concentrations, often remaining depressed at the end of the hydrograph. This pattern was typical of TN, NO_3^-, SEC, and pH (Figs. 4d, 6c). One additional, unusual pattern was observed for NO_3^- during three storm events in the summer of 2007 during an extended drought when concentrations of NO_3^- initially decreased on the rising limb of the
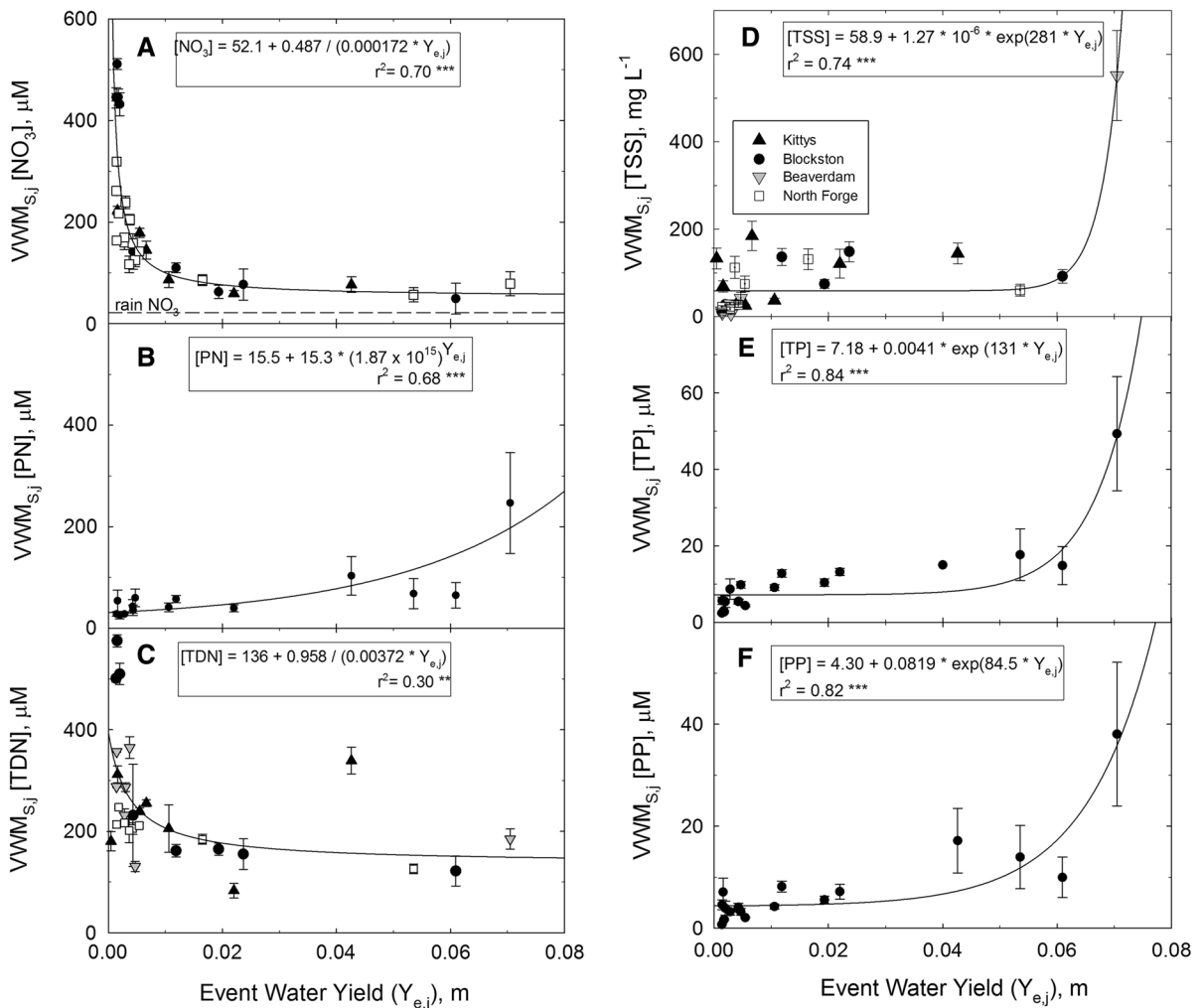
Fig. 9 Relationships between stormflow volume weighted mean concentrations ($VWM_{S,j}$) and event water yield ($Y_{e,j}$) for various N constituents (**a**–**c**), TSS (**d**), and two P constituents (**e**, **f**). Error bars are standard errors of the mean

hydrograph, but then atypically increased sharply during the falling limb.

Results of the timing of peak nutrient concentrations are presented in Table 4. In general, TSS, PP, and PN peaked 2–5 h before discharge on the rising limb, except at Blockston where particulates lagged 6–8 h after peak discharge. PO_4^{3-}, NO_3^-, and SEC tended to peak < 1–9 h after the discharge peak on the falling limb. PO_4^{3-} peaked before the NO_3^- nadir at the Kitty's Corner and Blockston watersheds, but followed the NO_3^- nadir at Beaverdam and North Forge watersheds. In general, time delays for smaller storms were longer than for larger storms.

Chemical concentrations (C) varied asymmetrically with discharge (Q) during storm events in C-Q patterns which are commonly observed (e.g., Chanat et al. 2002, see Fig. 7). NO_3, SEC, and TSS followed a clock-wise pattern, indicating higher concentrations on the rising limb (Fig. 7a), while PO_4^{3-} and, to a lesser extent, TP followed a counter clock-wise pattern (i.e. lower concentrations on the rising limb, Fig. 7b).

The chemistry of stormflow was found to be very different from that of baseflow (Figs. 4d, 6, 7, 8). Although NO_3^- declined during storm events, TN changed little due to increases in DON, PN, and NH_4^+. Despite variability in the sampled storm sizes, NH_4^+, TSS, PO_4^{3-}, and TP were higher during stormflows. For example, at the Kitty's Corner watershed, NH_4^+ was < 4 μM in baseflow samples compared to $VWM_{S,j}$ values of 17 μM in the storm samples (Fig. 8c, d). Nitrate concentrations during stormflows were 50–75% lower than in baseflow at all four watersheds (Figs. 6c, 8c, d). The measured TSS concentrations were 1–14 g m^{-3} in the baseflow samples compared to 50–100 g m^{-3} during stormflow. However, SEC was higher in baseflow, although only because of higher NO_3^- concentrations driving higher SEC. However, there were no consistent, significant differences in pH between the baseflow and stormflow samples.

Phosphorus concentrations, in particular, were found to be higher in the stormflow samples (Fig. 8a, b). For example, at the Beaverdam watershed, baseflow PO_4^{3-} concentrations were about 1 μM compared to stormflow concentrations of ~ 5 μM (Figs 8a, b). Similarly, stormflow concentrations of TP ranged from 4 to 11 times higher in the storm samples. For example, at the Beaverdam watershed, baseflow concentrations of TP were about 2 μM

compared to 22 μM in stormflow. The composition of TP also varied. At the well-drained Kitty's Corner and Blockston watersheds, baseflow TP consisted mainly of PO_4^{3-} (70% at Kitty's Corner and 51% at Blockston), while at the poorly drained Beaverdam and North Forge watersheds, baseflow TP was primarily composed of dissolved and particulate organic P (DOP + PP, 72%; Fig. 8a). During stormflows, TP at the four watersheds was mainly in particulate form (mean 65%), followed by PO_4 (mean 25%) and DOP (mean 10%, Fig. 8b).

The baseflow and stormflow samples also showed major differences in nitrogen composition (Fig. 8c, d). Although there were variations in baseflow TN concentrations among the watersheds, the composition of baseflow TN was consistently dominated by NO_3^- (mean 87%) at all four watersheds (Fig. 8c). In stormflows, NO_3^- was a smaller fraction of TN (mean 60%), but TN concentrations changed little due to increases in PN (mean 22%) and DON (mean 17%) during stormflow (Fig. 8c, d). This is a striking difference compared to TP concentrations, which were much higher during stormflows at all four watersheds (Fig. 8a, b).

Controls on stormflow chemistry

In the four Choptank watersheds, total event water yields (baseflow + stormflow, $Y_{e,j}$) were strongly correlated with the stormflow volume-weighted mean concentrations ($VWM_{S,j}$) of N (Fig. 9a–c), TSS (Fig. 9d), and P (Fig. 9e, f). The relationships between event water yield ($Y_{e,j}$, m) and $VWM_{S,j}$ for NO_3^- decreased hyperbolically with increasing event water yield ($r^2 = 0.70***$, Fig. 9a) down to 52 μM, or about twice the long-term rainfall mean of 22 μM for the Delmarva region (Scudlark et al. 1998). $VWM_{S,j}$ for NO_3^- was also linearly and positively correlated with mean event stream temperature ($T_{e,j}$ $r^2 = 0.41**$), although this term was not significant in a multivariate model with $Y_{e,j}$, probably because large events tend to occur at cooler temperatures. $VWM_{S,j}$ for PN increased exponentially with event water yield ($r^2 = 0.68***$, Fig. 9b) and was as high as 250 μM during the largest storm. $VWM_{S,j}$ for TDN decreased with event water yield ($r^2 = 0.30**$) in a manner similar to that of NO_3^- (Fig. 9c), but with more outliers which resulted in a weaker relationship. The similarity of the TDN and NO_3^- relationship with $Y_{e,j}$

Table 5 Total annual discharge and annual export coefficients (Y) of total nitrogen (TN), total phosphorus (TP), and total suspended sediment (TSS)

	Kitty's Corner	Blockston	Beaverdam	North Forge	Average
Includes storm samples					
Annual discharge (m year^{-1})	0.57	0.39	0.59	0.48	0.51 ± 0.04
% Stormflow	51	58	22	32	41 ± 8
Exp coef TN (kg ha^{-1} year^{-1})	26.9	25.7	32.8	21.9	27 ± 2
% Stormflow	48	25	16	30	30 ± 7
Exp coef TP (kg ha^{-1} year^{-1})	1.40	1.04	0.94	0.89	1.1 ± 0.1
% Stormflow	89	91	71	80	83 ± 5
Exp coef TSS (kg ha^{-1} year^{-1})	416	242	659	1140	610 ± 190
% Stormflow	99.7	99.4	99.6	99.9	99.6 ± 0.1
No storm samples					
Exp coef TN (kg ha^{-1} year^{-1})	26.2	29.8	21.0	14.5	23 ± 3
% decrease in TN export	− 3	+ 16	− 36	− 34	− 14 ± 13
Exp coef TP (kg ha^{-1} year^{-1})	0.34	0.16	0.24	0.17	0.23 ± 0.04
% decrease in TP export	− 76	− 85	− 74	− 19	− 64 ± 15
Exp coef TSS (kg ha^{-1} year^{-1})	23.7	15.6	23.6	17.9	20.2 ± 2.0
% decrease in TSS export	− 94	− 94	− 96	− 98	96 ± 1

Export coefficients of TN, TP, and TSS were calculated with storm samples (upper rows) and without storm samples (lower rows). For export including storm samples, the percentages of the annual export of water, N, and P in stormflow are shown for the four study watersheds with adequate chemistry data. For export without storm samples, the annual export coefficients were calculated based only on monthly baseflow chemistry samples and total flow data, with the decrease in export shown. At Blockston, estimating export without storm samples caused an overestimation of export because of large decreases in TN during storms

is expected because TDN is mostly NO_3^- (Fig. 8). $VWM_{S,j}$ for NH_4^+ was linearly and inversely related to event stream temperature $T_{e,j}$ ($r^2 = 0.23^{**}$, not shown). Because of opposing effects of event water yield on NO_3^- and PN, $VWM_{s,j}$ for TN was not significantly related to event water yields or temperature.

The $VWM_{S,j}$ of TSS in the storm samples increased exponentially with event water yield $Y_{e,j}$ ($r^2 = 0.74^{***}$, Fig. 9d). This figure illustrates the increase in soil erosion and sediment re-suspension as storm size increases, although this relationship is primarily due to the highest $VWM_{S,j}$ measured for TSS (550 g m^{-3}) during the large April 2007 storm at the Beaverdam watershed. The same storm event was also measured at the other watersheds, but with lower $Y_{e,j}$ values and only moderate $VWM_{S,j}$ values (60–144 g m^{-3}). These differences illustrate the highly site-specific nature of precipitation, storm flow, and sediment mobilization during storm events in the Choptank watersheds.

Volume-weighted mean concentrations of $VWM_{S,j}$ for P were also significantly related to event water yields. $VWM_{S,j}$ of TP increased exponentially with event water yield ($r^2 = 0.84^{***}$, Fig. 9e), reflecting the mobilization of P during storm events. TP was also inversely related to $T_{e,j}$ ($r^2 = 0.24^*$), but adding temperature to the regression between $Y_{e,j}$ and TP did not significantly improve the relationship. $VWM_{S,j}$ for PP increased exponentially with event water yield ($r^2 = 0.82^{***}$, Fig. 9f) to a maximum of ∼ 40 μM during high discharge associated with the April 2007 storm. $VWM_{s,j}$ for PO_4^{3-} was not significantly related to event water yield or temperature.

pH and SEC were significantly related to $Y_{e,j}$ and $T_{e,j}$. $VWM_{S,j}$ of pH increased linearly with mean event stream temperature $T_{e,j}$ ($r^2 = 0.29^{**}$), an effect that may be due to soil liming at colder temperatures in spring when fields are being prepared for crops. $VWM_{S,j}$ of SEC decreased with event water yield to a level that is about three times the long-term rainfall mean (data not shown but virtually identical to NO_3^-

Fig. 10 Relationships between annual stormflow (**a**) and annual baseflow (**b**) with mean watershed slope for the combined USGS and Choptank data set
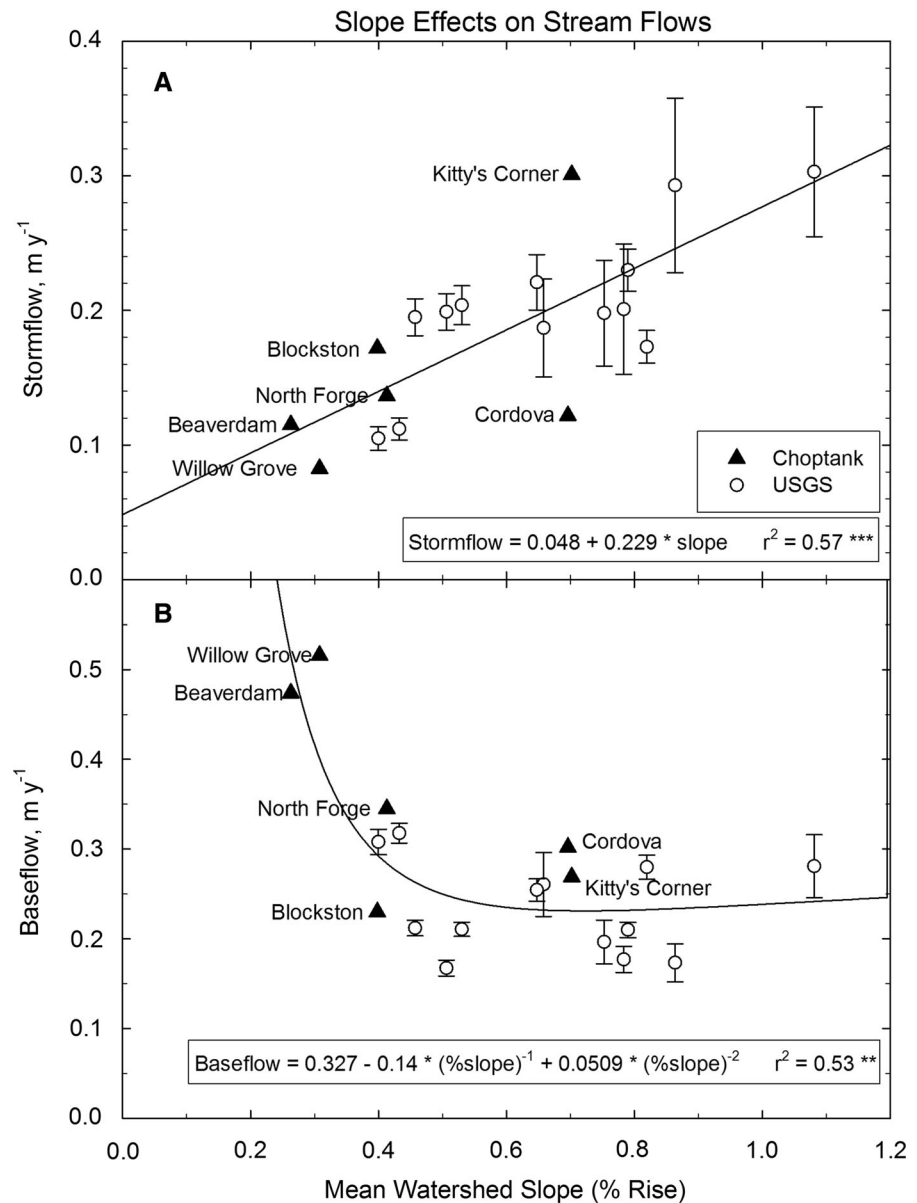
in Fig. 9a). The similarity to the NO_3^- curve is due to the fact that SEC is largely driven by variations in NO_3^-, a major ion in streams draining agricultural watersheds.

Annual export of nutrients and sediment

The relationships between $VWM_{S,j}$ of N, P, and TSS, and storm event water yields (Fig. 9) were used for estimating export during unsampled storms. Export during all storms is important for calculating the total

annual export of nutrients and sediment from the Choptank watersheds. All of the relationships were strong and statistically significant, ranging from $r^2 = 0.68^{***}$ to 0.84^{***} for the different constituents with the exception of TDN which was significant but had a lower r^2 value (0.30^{**}). The scatter in the TDN data was due to the fact that NH_4^+ and DON were generally less predictable in stormflows compared to TSS, TP, and NO_3^-. The TN concentration for unsampled storms was estimated as TDN (Fig. 9c)

plus PN (Fig. 9b), and $VWM_{S,j}$ for TN in sampled storms was computed directly from Eq. 3.

The calculated annual export coefficients for TN, TP, and TSS (Y, kg ha^{-1} year^{-1}) are summarized in Table 5. The annual export coefficients (kg ha^{-1} year^{-1}) ranged as follows: TN = 22–33 (mean = 27 $\pm$ 2), TP = 0.9–1.4 (mean = 1.1 $\pm$ 0.1), and TSS = 242–1140 (mean = 610 $\pm$ 190). By separating base and stormflow volumes and chemistry, it was found that 99% of the total annual TSS export, 71–91% of the total annual TP export, and 16–48% of the total annual TN export occurred during periods of stormflow (Table 5), while the remainder occurred during baseflow. For comparison, stormflow volumes were 22–58% (mean = 41 $\pm$ 8%) of the total annual discharge volumes from the watersheds. The smaller impact of stormflows on N export is due to lower nitrate and TDN concentrations during higher discharges (Fig. 9a, c).

Discussion

Test of the hypothesis

The hypothesis of this study was that watersheds with larger amounts of poorly-drained hydric soils generate more storm discharge compared to watersheds with well-drained, non-hydric soils. The data collected in the Choptank watersheds (Fig. 5, Table 5) showed no significant correlation ($p > 0.10$) between percent hydric soils and annual stormwater yields, which did not support the hypothesis. However, due to the limited sample size of the Choptank stations (n = 6), we also tested the hypothesis more broadly with additional stream discharge data from 13 nearby USGS stream gauging stations on Delmarva (Koskelo 2008, see Fig. 1) to supplement the Choptank data. Combining the Choptank and USGS datasets (n = 19 watersheds) also did not show any statistically significant correlation between percent hydric soils and annual stormflow water yields, baseflow water yields, or total water yields ($p > 0.10$).

As an alternative hypothesis, we examined the role of mean watershed slope in the Choptank and USGS watersheds as a possible control on annual stormflow and baseflow water yields (m year^{-1}). Among the combined Choptank and USGS watersheds, the slopes ranged from 0.2 to 1.1%, which is typical for the relatively flat Atlantic coastal plain. The combined Choptank and USGS data showed that annual stormflow water yields increased linearly with average watershed slope ($r^2 = 0.57$***), despite differences in land use and hydric soils among the watersheds (Fig. 10a).

Baseflow water yields (m year^{-1}) were also found to be related to mean watershed slope for the combined Choptank and USGS data set. However, in this case, it was an inverse relationship, in which flatter slopes resulted in more baseflow. While the relationship in Fig. 10b was fairly strong, much of it depends on two of the Choptank watersheds (Beaverdam and Willow Grove, Fig. 10b), which have the lowest slopes and the highest baseflow water yields. Therefore, the effect of mean watershed slope on baseflow and stormflow needs further exploration with additional watersheds to expand the sample size.

It is intuitive that steeper watershed slopes could cause an increase in stormflow volumes, but there was little confirmation of this in the literature. At the watershed scale, Harlin (1984) suggested the use of hypsometry and watershed relief to increase the predictive power and transferability of rainfall-runoff models, and Rose and Peters (2001) showed that runoff as a fraction of precipitation was greatest at higher elevation and relief and decreased at lower elevation and relief at USGS gauges near Atlanta Georgia USA. The strongest supporting evidence comes from a study of urbanization in major US East Coast metropolitan areas by Hopkins et al. (2015) who noted that watershed slopes of 1–10% had significant effects on the timing and magnitude of stormflows and sometimes were more important than urbanization effects. There was also evidence for the importance of slope in generating storm runoff at smaller experimental scales; Haggard et al. (2005) found that slope was directly proportional to the volume of overland flow in a controlled mesocosm experiment, and a study by Hopp and McDonnell (2009) likewise determined that higher slope angles caused an increase in storm flows in a calibrated, finite-element model.

The data in Fig. 10 are consistent with the concept that precipitation falling on watersheds with low slopes tends to pond rather than run off into surface waters, resulting in relatively little stormflow response in the stream (Fig. 10a). These ponded areas are known locally as "Delmarva Bays" and are visible across the landscape following a storm, usually in

small depressions of 10–100 m in diameter associated with hydric soils. Based on the streamflow measurements in Fig. 10, it is inferred that some of the ponded water in these Delmarva Bays may evaporate, while the rest slowly infiltrates to groundwater, enhancing baseflow at slopes < 0.4% (Fig. 10b). The reduced annual yields of stormflow associated with hydric soils suggests that these areas of ponding and slow infiltration within watersheds are not significant sources of N, P, and TSS due to the constrained hydrology induced by ponding.

Stormflow chemistry

During the 31 sampled storm events in the Choptank watersheds, there were three consistent relationships between discharge and N, P, and TSS concentrations. The first pattern was characterized by large but short-lived peaks in concentration exemplified by particulate N and P, and TSS (e.g., Fig. 6a). The peak concentrations of particulates were 10–100 times higher than typical baseflow concentrations. Particulates were rapidly transported to the streams at the start of the rising limb of the hydrograph. This was likely the result of physical erosion of upland soils, as well as scouring of the stream banks and re-suspended bedload from the bottom of the stream channel at greater water depths and faster flow velocities (Kuhnle et al. 1996; Correll et al. 1999; Thompson 2008). Most erosion occurred during the early portion of the storm, typically several hours before the discharge peak, and little to no erosion occurred after this, consistent with a clock-wise hysteresis pattern between concentration and discharge (Fig. 7a).

The second pattern was characterized by smaller but broader peaks in concentrations, as exhibited by NH_4^+ and PO_4^{3-} (e.g., Fig. 6b). The transport of these ions to the streams during storms was slower than the particulates, with concentrations of NH_4^+ nearly coincident with peak discharge and the PO_4^{3-} peak occurring 3–9 h after the discharge peak (Table 4). This reflects the gradual release of soil PO_4^{3-} and NH_4^+ from the watershed over the course of a storm event. The low PO_4^{3-} concentrations on the rising limb and higher concentrations on the falling limb (opposite to that of particulates) is consistent with a counter-clockwise hysteresis (Fig. 7b). PO_4^{3-} and NH_4^+ generally have strong affinities for the soil matrix and therefore bind to soil particles. However,

through chemical desorption processes triggered by infiltrating precipitation and soil saturation, they appear to be gradually released from the soil and eventually drain to the stream toward the middle and end of the storm.

The third pattern was a decrease in concentrations during the storm event followed by a gradual increase back to pre-storm, baseflow concentrations. The constituents which followed this pattern included SEC, pH, and NO_3^-. In the case of NO_3^-, concentrations slowly decreased at the beginning of the storm and did not reach the nadir concentration (which averaged 50–70% of typical baseflow concentrations) until much later in the storm, 4.5 ± 1.0 h after peak discharge (Table 4). The depressed NO_3^- concentrations were the result of in-stream dilution, in which the relatively high NO_3^- concentrations in groundwater (Fox et al. 2014) were diluted by much lower concentrations in rain (Scudlark et al. 1998) and in overland and sub-surface flows. However, the decrease in NO_3^- concentrations was offset by increases in PN and DON concentrations (Fig. 8), resulting in relatively small changes in TN concentrations during an event. Following the nadir, NO_3^- concentrations very slowly rebounded and did not return to pre-storm levels until well after the storm had ended (e.g. Figure 6b, 7a).

These patterns of C-Q hysteresis are similar to those reported elsewhere. For example, in the classification of C-Q responses developed by Chanat et al. (2002), the examples in Fig. 7 fall into their C3 and A2 groups, where event concentrations fall between those in groundwater and soil water for NO_3^- and PO_4^{3-}, respectively, indicating differing mixtures of water sources during the event. Our data are also consistent with other studies reported in the literature (Vanni et al. 2001; Gachter et al. 2004; Volk et al. 2006; Sharpley et al. 2008), but not all (O'Brien et al. 1993; Correll et al. 1999; Kline et al. 2007). As an example of the latter, Correll et al. (1999) found that both PO_4^{3-} and NO_3^- concentrations changed little during storm discharges in nearby watersheds of the Rhode River in central MD, on the inner edge of the Mid-Atlantic coastal plain. Other dissimilar findings are reported in O'Brien et al. (1993) and Kline et al. (2007), who found that NO_3^- concentrations consistently increased during storm discharges in watersheds of the Appalachian Plateau in western MD. These differences are most likely due to regional variations;

i.e., the watersheds studied by Correll et al. (1999) are much smaller and steeper than those in the Choptank, and the O'Brien et al. (1993) and Kline et al. (2007) studies took place in a region of MD with very different soils, geology, and terrain.

On the other hand, studies by Vanni et al. (2001) and Volk et al. (2006) report very similar patterns of in-stream constituent concentrations. In our study, NO_3^- concentrations were consistently lower in stormflows compared to baseflows during 28 of the 31 sampled storm events (Figs. 6, 7, 8). However, there were three atypical storms following hot dry periods in which NO_3^- concentrations initially increased sharply during the early part of the storm but then reverted to the usual pattern (i.e. depressed concentrations followed by a long gradual return to pre-storm concentrations). Vanni et al. (2001) observed the same pattern for NO_3^- following extended drought periods in agricultural watersheds in the mid-western U.S. In both this study and Vanni et al. (2001), we speculate that NO_3^- in the upper soil layers accumulated to abnormally high levels during a prolonged drought. The crops may have been unable to utilize NH_4^+ produced in the soil and from fertilizer N, resulting in NO_3^- accumulation in the soil. At the first significant rainfall following this dry period, the large store of soil NO_3^- may have been flushed rapidly into the streams via soil macropores or overland flow, resulting in a large increase in stream NO_3^- concentrations. Following this initial flush, the normal dilution of high-NO_3^- baseflow with low-NO_3^- storm runoff may have resumed. Testing this concept is a useful direction for future research on stormflow chemistry and the influence of droughts. Notably, both the Vanni et al. (2001) and Volk et al. (2006) studies included watersheds that are very similar to the Choptank watersheds studied here in terms of land use (agriculturally-dominated) with low slopes. This suggests that it is possible for small, intensively farmed watersheds with comparable slopes to exhibit similar patterns of in-stream NO_3^- concentrations during storm events, even if the watersheds are widely distributed over a large geographic region.

Composition of N and P in storm discharges

In this study, TN during storm discharges was composed of the following N species in order of decreasing abundance: NO_3^- ($\sim 60\%$ of TN on average), PN ($\sim 20\%$), DON ($\sim 15\%$), and NH_4^+ ($\sim 5\%$, see Fig. 8). The relatively small contributions of DON and NH_4^+ is consistent with similar studies by Sutton et al. (2009), Correll et al. (1999), and Volk et al. (2006). However, in the latter two studies, NO_3^- was a much smaller fraction of TN ($< 30\%$) while PN was a much higher fraction ($> 80\%$), indicating that the composition of TN across studies is similar in some respects but not all. Importantly, while the composition of TN changes greatly during storm discharges, the absolute TN concentrations change very little (Fig. 8).

TP in storm discharges was dominated by particulate P, which represented 65% of the TP on average. Correll et al. (1999) and Sutton (2006) also found that P transport during storms is dominated by particulate forms. However, Primrose et al. (1997) found that PO_4^{3-}, not particulates, was the dominant form of P in storm discharges of the German Branch watershed (also in the Choptank Basin). It is unclear why this would be the case, unless it is due to differences in sampling programs or unique conditions within the German Branch watershed which are not representative of the other Choptank watersheds.

Annual export of nutrients and sediment

Annual export coefficients (kg ha^{-1} year^{-1}) of TN, TP, and TSS from the Choptank watersheds ranged from 22 to 33 for TN, from 0.9 to 1.4 for TP, and from 242 to 1140 for TSS (top of Table 5). Of these totals, 16–48% of the TN, 22–58% of the water, 71–91% of the TP, and 99% of the TSS was exported during periods of stormflow while the remainder was exported during baseflow. The export coefficients reported here for mixed landuse watersheds dominated by agriculture are generally on the low end compared to those reported in the literature. Vanni et al. (2001) summarized TN and TP annual export coefficients from 10 studies of row-crop agriculture. They found that nutrient coefficients (kg N or P ha^{-1} year^{-1}) vary widely, from 2.1 to 80 for TN and from 0.1 to 18.6 for TP. They attributed this large variability to wide geographic distributions and differences in sampling programs. The Choptank export coefficients were also compared to those of the nearby USGS stream gauging station at Greensboro (48% agriculture, Fig. 1), where annual export (kg ha^{-1} year^{-1}) ranged from 2.9 to 11.5 for TN and from 0.1 to 0.7 for TP during

1981–1990 (Fisher et al. 1998). The export coefficients of the Choptank watersheds are higher because they have more agricultural land use (65–76%, Table 1), which is a major driver of N and P export on Delmarva (Fisher et al. 2006, 2010).

As indicated above, the annual export coefficients for the Choptank watersheds are dominated by stormflows, especially for TP and TSS, while baseflow is less important. Clearly, storm sampling is a critical part of a watershed monitoring program if reasonable estimates of annual nutrient and sediment export are desired. To determine how much of the annual export would (hypothetically) be missed if only baseflow sampling were conducted, we re-calculated the annual exports without including the storm chemistry data (i.e., baseflow chemistry applied to storm volumes). The results indicate that (on average) 79% of the TP, 95% of the TSS, and 14% of the TN would be missed if no storm samples were collected (bottom of Table 5). The reason why only a small amount of TN would be missed is because the absolute TN concentrations change relatively little between base and storm flows, although the composition of TN changes markedly during storm events (Fig. 8).

Controlling factors

In this study, the VWM concentrations of N, P, and TSS during storm discharges were found to vary with event water yields (Fig. 9). This indicates that the total discharge volume of a particular storm event is a useful predictor of in-stream nutrient and sediment concentrations. For PN, TDN, TP, PP, and TSS, larger storms were associated with higher VWM concentrations, while for NO_3^- and TDN, larger storms resulted in lower VWM concentration. Exponential or hyperbolic functions were found to best describe the relationships between VWM concentrations and event water yields, and these relationships were generally highly significant. Since the 31 sampled events included in this study were distributed across all seasons, and no strong relationships were found between VWM concentrations and event water temperature, it appears that any seasonal effects are secondary to flow volumes in controlling in-stream nutrient and sediment concentrations during storms. Due to fortuitous weather patterns during the 15-month monitoring period, several large storms, including two extreme events, were sampled, allowing us to populate the upper end of the exponential or hyperbolic curves. This provided a strong basis for using the relationships in Fig. 9 to estimate contributions from unmeasured storms to annual export of N, P, and TSS.

The observed increase in TSS VWM concentrations with larger storms is consistent with well-established principles of the geomorphology of alluvial streams (Wolman and Miller 1960). The rate of sediment scouring from the channel bed and banks can be expressed as a power function of shear stress, similar to the curve shown in Fig. 9d. While moderate flows have some erosive capacity, it is the larger, less frequent storm events that cause the most erosion, resulting in higher in-stream TSS concentrations. While some studies (e.g. Sharma et al. 2012) have found that TSS VWM concentrations are also highly correlated with rainfall characteristics (such as total rainfall depth or rainfall intensity), no such relationship was found here. One local study by Jordan et al. (1997a) found that flow-weighted mean concentrations of TSS and P are correlated to each other. This suggests that TSS and P are co-variates in storm runoff (compare Fig. 9d with 9e), as P is often adsorbed to sediment particles in the soil matrix. In a study of agricultural watersheds in the Susquehanna Basin, the largest freshwater source for Chesapeake Bay, Sharpley et al. (2008) found strong correlations ($r^2 = 0.98*$) between stormflow P concentrations and the stormflow return period, a proxy for event volume. In agricultural watersheds in Alberta, Canada, Casson et al. (2008) found that TN concentrations in runoff were strongly ($r^2 = 0.68–0.72***$) and positively related to extractable NO_3-N concentrations (mg kg^{-1}) in the uppermost soil layers (0–10 cm in depth). Overall, these studies suggest that there are multiple factors that control stormwater VWM concentrations of N, P, and TSS in agricultural watersheds, ranging from precipitation to stream discharge to soil characteristics. In this study, stream discharge (expressed as event water yield), was found to be the primary driver for many of the measured nutrient fractions and sediment.

Conclusions

The hypothesis that hydric soils promote overland flows due to limited soil permeability was not supported by our data. In contrast we show that

stormflows are promoted by watershed slope, based on evidence from 19 watersheds, including both the Choptank watersheds and nearby USGS stream gauging stations on the Delmarva Peninsula (Fig. 10a). In contrast, baseflow was relatively independent of mean watershed slope, except for the two watersheds with the lowest slopes and most hydric soils (Fig. 10b). This small interaction of hydric soils and watershed slope suggests that mean watershed slope has little effect on baseflow, except at very low slopes where ponding on hydric soils may limit stormflow and increase long-term infiltration and baseflow.

The results of this study show the importance of sampling stormflows to quantify watershed export. Seventy-one to 99% of annual P and TSS transport, but only 16–48% of annual N transport, occured during brief periods of storm runoff in small, agriculturally-dominated watersheds. Particulate forms of N and P, as well as TSS, increase ten-fold relative to baseflow during the initial runoff period, likely due to physical scouring of the stream bed and banks, as well as erosion of adjacent soils that are disturbed by agricultural practices. From peak discharge to the end of the storm, particulates decrease in the stream, having been washed out in the first flush. For TP and TSS, major storms are critical times of export, as during these events, concentrations can increase ten-fold and export rates can be orders of magnitude higher.

Finally, the relationships between VWM concentrations of N, P, and TSS, and event water yields can be used as a tool to estimate annual export of nutrients and sediment. Extending these relationships to other regions could potentially incorporate other empirical parameters beyond storm volume (e.g., precipitation characteristics, landuse, latitude) as predictors of VWM concentrations in a multi-parameter approach. If validated elsewhere, this approach can potentially provide a useful means of incorporating stormflow into estimates of annual nutrient and sediment export with continuous hydrology measurements but limited storm sampling.

References

Aguilera R, Melack JM (2018) Concentration-discharge responses to storm events in coastal California watersheds. Water Resour Res 54:407–424

Akaike H (1973) Information theory as an extension of the maximum likelihood principle. In: Petroy BN, Csaki F (eds) Second international symposium on information theory. Akademiai Kiado, Budapest, pp 267–281

Andersen JM (1976) An ignition method for determination of total phosphorus in lake sediments. Water Res 10:329–331

Basu NB, Destouni G, Jawitz JW, Thompson SE, Loukinova NV, Darracq A, Zanardo S, Yaeger M, Sivapalan M, Rinaldo A, Rao PSC (2010) Nutrient loads exported from managed catchments reveal emergent biogeochemical stationarity. Geophys Res Lett 37:L23404

Beckert KA, Fisher TR, O'Neil JM, Jesien RV (2011) Characterization and comparison of stream nutrients, land use, and loading patterns in Maryland Coastal Bay watersheds. Water Air Soil Pollut 221:255–273

Buffam IJN, Galloway L, Blum K, McGlathery KJ (2001) A stormflow/baseflow comparison of dissolved organic matter concentrations and bioavailability in an Appalachian stream. Biogeochemistry 53:269–306

Burnham KP, Anderson DR (2002) Model selection and multimodal inference: a practical information-theoretic approach, 2nd edn. Springer, New York

Casson, JP, Olson BM, Little JL, Nolan SC (2008) Assessment of environmental sustainability in Alberta's AgriculturalWatersheds Project, vol 4. Nitrogen loss in surface runoff. Alberta Agricultural and Rural Development, Lethbridge

Chanat JG, Rice KC, Hornberger GM (2002) Consistency of patterns in concentration-discharge plots. Water Res Res 38:22-1–22-10

Correll DL, Jordan TE, Weller DE (1995) Livestock and pasture land effects on the water quality. In: Steele K (ed) Animal waste and the land–water interface. Lewis Publisher, New York, pp 107–117

Correll DL, Jordan TE, Weller DE (1999) Transport of nitrogen and phosphorus from Rhode River watersheds during storm events. Water Resour Res 35:2513–2521

Denver JM, Ator SW, Debrewer LM, Farrari J, Barbaro JR, Hancock TC, Brayton MJ, Nardi MR (2004) water Quality in the Delmarva Peninsula, Delaware, Maryland, and Virginia, 1999–2001. USGS Circular 1228

Federal Register (1994) Changes in hydric soils of the United States, vol 59(33). Department of Agriculture, Soil Conservation Service, United States Department of Agriculture, Washington DC

Fisher TR, Lee KY, Berndt H, Benitez JA, Norton MM (1998) Hydrology and chemistry of the Choptank River Basin. Water Air Soil Pollut 105:387–397

Fisher TR, Hagy JD, Boynton WR, Williams MR (2006) Cultural eutrophication in the Choptank and Patuxent estuaries of Chesapeake Bay. Limnol Oceanogr 51:435–447

Fisher TR, Jordan TE, Staver KW, Gustafson AB, Koskelo AI, Fox RJ, Sutton AJ, Kana T, Beckert KA, Stone JP, McCarty G, Lang M (2010) The Choptank Basin in transition: intensifying agriculture, slow urbanization, and estuarine eutrophication. In: Kennish MJ, Paerl HW (eds), Coastal lagoons: systems of natural and anthropogenic change. CRC Press, pp 135-165

Focazio MJ, Cooper RE (1995) Selected characteristics of stormflow and baseflow affected by land use and cover in the Chickahominy River Basin, Virginia, 1989–1991. U.S. Geological Survey Water-Res. Invest. Rep. 94-4225

GOM Watershed Nutrient Task Force (2001) Action plan for reducing, mitigating, and controlling hypoxia in the Northern Gulf of Mexico. https://www.epa.gov/ms-htf/hypoxia-task-force-2001-action-plan

Fox RJ, Fisher TR, Gustafson AB, Jordan TE, Kana TM, Lang MW (2014) Searching for the missing nitrogen: biogenic nitrogen gases in groundwater and streams. J Agric Sci 152:S96–S106

Gachter R, Steingruber SM, Reinhardt M, Wehrli B (2004) Nutrient transfer from soil to surface waters: differences between nitrate and phosphate. Aquat Sci 66:117–122

Gonzalez-Hidalgo JC, Batalla RJ, Cerda A (2013) Catchment size and contribution of the largest daily events to suspended sediment load on a continental scale. CATENA 102:40–45

Groffman PM, Bain DJ, Band LE, Belt KT, Brush GS, Grove JM, Pouyat RV, Yesilonis IC, Zipperer WC (2003) Down by the riverside: urban riparian ecology. Front Ecol Environ 1:315–321

Haggard BE, Moore PA Jr, Brye KR (2005) Effect of slope on runoff from a small variable slope box-plot. J Environ Hydrol 13:1–8

Hamilton PA, Denver JM, Phillips PJ, Shedlock RJ (1993) Water-quality assessment of the Delmarva Peninsula, Delaware, Maryland, and Virginia—effects of agricultural activities on, and distribution of, nitrate and other inorganic constituents in the surficial aquifer. US Geological Survey Open-File Report 93-40

Harlin JM (1984) Watershed morphometry and time to hydrograph peak. J Hydrol 67:141–154

Hopkins KG, Morse NB, Bain DJ, Bettez ND, Grimm NB, Morse JL, Palta MM, Shuster WD, Bratt AR, Suchy AK (2015) Assessment of regional variation in streamflow responses to urbanization and the persistence of physiography. Environ Sci Technol 49:2724–2732

Hopp L, McDonnell JJ (2009) Connectivity at the hillslope scale: identifying interactions between storm size, bedrock permeability, slope angle, and soil depth. J Hydrol 376:378–391

Jordan TE, Correll DL, Weller DE (1997a) Effects of agriculture on discharges of nutrients from coastal plain watersheds of Chesapeake Bay. J Environ Qual 26:836–848

Jordan TE, Correll DL, Weller DE (1997b) Nonpoint source discharges of nutrients from Piedmont watersheds of Chesapeake Bay. J Am Water Resour Assoc 33:631–645

Jordan TE, Correll DL, Weller DE (1997c) Relating nutrient discharges from watersheds to landuse and streamflow variability. Water Res Res 33:2579–2590

Kemp WM, Boynton WR, Adolf JE, Boesch DF, Boicourt WC, Brush G, Cornwell JC, Fisher TR, Glibert PM, Hagy JD, Harding LW, Houde ED, Kimmel DG, Miller WD, Newell RIE, Roman MR, Smith EM, Stevenson JC (2005) Eutrophication of Chesapeake Bay: historical trends and ecological interactions. Mar Ecol Prog Ser 303:1–29

Kline KM, Eshleman KN, Morgan RP, Castro NM (2007) Analysis of trends in episodic acidification of streams in western Maryland. Environ Sci Technol 41:5601–5607

Koskelo AI (2008) Hydrologic and biogeochemical storm response in Choptank Basin headwaters. Master's Thesis, University of Maryland

Koskelo AI, Fisher TR, Utz R, Jordan TE (2012) A new precipitation-based method of baseflow separation and event identification for small watersheds (< 50 km^2). J Hydrol 450–451:267–278

Kuhnle RA, Bingner RL, Foster GR, Grissinger EH (1996) Effect of land use changes on sediment transport. Water Resour Res 32:3189–3196

Lee KY, Fisher TR, Rochelle-Newall E (2001) Modeling the hydrochemistry of the Choptank River Basin using GWLF and Arc/Info: 2. Model validation and application. Biogeochemistry 56:311–348

McCarty GW, McConnell LL, Hapeman CJ, Sadeghi A, Graff C, Hively WD, Lang MW, Fisher TR, Jordan T, Rice CP, Codling EE, Whitall D, Lynn A, Keppler J, Fogel ML (2008) Water quality and conservation practice effects in the Choptank River watershed. J Soil Water Conserv 63:461–474

Moatar F, Abbott BW, Minaudo C, Curie F, Pinay G (2017) Elemental properties, hydrology, and biology interact to shape concentrations-discharge curves for carbon, nutrients, sediment, and major ions. Water Resour Res 53:1270–1287

Mohamoud YM (2010) Prediction of daily flow duration curves and streamflow for ungauged catchments using regional flow duration curves. Hydrol Sci J 53:706–724

Musolff A, Fleckenstein JH, Rao PSC, Jawitz JW (2017) Emergent archetype patterns of coupled hydrologic and biogeochemical responses in catchments. Geophys Res Lett 44:4143–4151

NAS (2000) Clean coastal waters. Understanding and reducing the effects of nutrient pollution. http://www.nap.edu/catalog/9812.html

Norton MGM, Fisher TR (2000) The effects of forest on stream water quality in two coastal plain watersheds of the Chesapeake Bay. Ecol Eng 14:337–362

Norvell WA, Frink CR, Hill DE (1979) Phosphorus in Connecticut lakes predicted by land use. Proc Natl Acad Sci 76:5426–5429

Novotny V, Sung H-M, Bannerman R, Baum K (1985) Estimating nonpoint pollution from small urban watersheds. J Water Pollut Control 57:339–348

O'Brien AK, Rice RC, Kennedy MM (1993) Comparison of episodic acidification of Mid-Atlantic upland and coastal plain streams. Water Res Res 29:3029–3039

Phillips PJ, Denver JM, Shedlock RJ, Hamilton PA (1993) Effect of forested wetlands on nitrate concentrations in

ground water and surface water on the Delmarva peninsula. Wetlands 13:75–83

Pionke HB, Gburek WJ, Sharpley AN, Schnabel RR (1996) Flow and nutrient export patterns for an agricultural hill-land watershed. Water. Res. Res. 32:1795–1804

Pionke HB, Gburek WJ, Sharpley AN (2000) Critical source area controls on water quality in an agricultural watershed located in the Chesapeake Basin. Ecol Eng 14:325–335

Pitt R, Chen S-E, Clark S (2004) Compacted urban soils effects on infiltration and bioretention stormwater control designs. In: Proceedings of 9th international conference on urban drainage, 8–13 September 2002, Portland OR, USA

Powers SM, Bruulsema TW, Burt TP, Chan NL, Elser JJ, Haygarth PM, Howden NJK, Jarvie HP, Lyu Y, Peterson HM, Sharpley AN, Shen J, Worrall F, Zhang F (2016) Long-term accumulation and transport of anthropogenic phosphorus in three river basins. Nat Geosci. https://doi.org/10.1028/ngeo2693

Press WH, Teukolsky S, Vetterling WT, Flannery B (2007) Numerical recipes in C: the art of scientific computing, 3rd edn. Cambridge University Press, New York

Primrose NL, Millard CJ, McCoy JL, Dobson MG, Sturm PE, Bowen SE, Windschitl RJ (1997) German Branch targeted watershed project: biotic and water quality monitoring evaluation report 1990–1995. Maryland Department of Natural Resources Report No. CCWS-WRD-MN-97-03

Rose S, Peters NE (2001) Effects of urbanization on streamflow in the Atlantia area (Georgia, USA): a comparative hydrological approach. Hydrol Process 15:1441–1457

Scudlark JR, Russell KM, Galloway JN, Church TM, Keene WC (1998) Organic nitrogen in precipitation at the mid-Atlantic U.S. coast—methods evaluation and preliminary measurements. Atmos Environ 32:1719–1928

Sharma D, Gupta R, Singh RK, Kansal A (2012) Characteristics of the event mean concentration (EMCs) from rainfall runoff on mixed agricultural land use in the shoreline zone of the Yamuna River in Delhi, India. Appl Water Sci 2:55–62

Sharpley AN, Kleinman PJA, Heathwaite AL, Gburek WJ, Folmar GJ, Schmidt JP (2008) Phosphorus loss from an agricultural watershed as a function of storm size. J Environ Qual 37:362–368

Shields CA, Band LE, Law N, Groffman PM, Kaushal SS, Savvas K, Fisher GT, Belt KT (2008) Streamflow distribution of non-point source nitrogen export from urban-rural catchments in the Chesapeake Bay watershed. Water Resour Res 44:W09416. https://doi.org/10.1029/2007wr006360

Strickland JDH, Parsons TR (1972) A practical handbook of seawater analysis, 2nd edn. Fisheries Research Board of Canada, Ottawa

Sutton AJ (2006) Evaluation of agricultural nutrient reductions in restored riparian buffers. Dissertation, University of Maryland

Sutton AJ, Fisher TR, Gustafson AB (2009) Historical changes in water quality at German Branch in the Choptank River Basin. Water Air Soil Pollut 199:353–369

Sutton AJ, Fisher TR, Gustafson AB (2010) Effects of restored stream buffers (CREP) on water quality in non-tidal streams in the Choptank River Basin. Water Air Soil Pollut 208:101–118

Thompson DM (2008) The influence of lee sediment behind large bed elements on bedload transport rates in supply-limited channels. Geomorphology 99:420–432

Valderrama JC (1981) The simultaneous analysis of total nitrogen and total phosphorus in natural waters. Mar Chem 10:109–122

Vanni MJ, Renwick WH, Headworth JL, Auch JD, Schaus MH (2001) Dissolved and particulate nutrient flux from three adjacent agricultural watersheds: a five-year study. Biogeochemistry 54:85–114

Volk JA, Savidge KB, Scudlark JR, Andres AS, Ullman WJ (2006) Nitrogen loads through baseflow, stormflow, and underflow to Rehoboth Bay, Delaware. J Environ Qual 35:1742–1755

Wolman MG, Miller JP (1960) Magnitude and frequency of forces in geomorphic processes. J Geol 68:54–74

Zar JH (1999) Biostatistical analysis, 4th edn. Prentice Hall, Singapore